

Automated Synthesis of Fault-Tolerant State Preparation Circuits for Quantum Error Correction Codes

Tom Peham,^{1,*} Ludwig Schmid,^{1,†} Lucas Berent,^{1,‡} Markus Müller,^{2,3,§} and Robert Wille^{1,4,¶}

¹Technical University of Munich

²Institute for Quantum Information, RWTH Aachen University, D-52056 Aachen, Germany

³Peter Grünberg Institute, Theoretical Nanoelectronics,
Forschungszentrum Jülich, D-52425 Jülich, Germany

⁴Software Competence Center Hagenberg, Austria

A central ingredient in fault-tolerant quantum algorithms is the initialization of a logical state for a given quantum error-correcting code from a set of noisy qubits. A scheme that has demonstrated promising results for small code instances that are realizable on currently available hardware composes a non-fault-tolerant state preparation step with a verification step that checks for spreading errors. Known circuit constructions of this scheme are mostly obtained manually, and no algorithmic techniques for constructing depth- or gate-optimal circuits exist. As a consequence, the current state-of-the-art exploits this scheme only for specific code instances and mostly for the special case of distance 3 codes. In this work, we propose an automated approach for synthesizing fault-tolerant state preparation circuits for arbitrary CSS codes. We utilize methods based on satisfiability solving (SAT) techniques to construct fault-tolerant state preparation circuits consisting of depth- and gate-optimal preparation and verification circuits. We also provide heuristics that can synthesize fault-tolerant state preparation circuits for code instances where no optimal solution can be obtained in an adequate timeframe. Moreover, we give a general construction for non-deterministic state preparation circuits beyond distance 3. Numerical evaluations using $d = 3$ and $d = 5$ codes confirm that the generated circuits exhibit the desired scaling of the logical error rates. The resulting methods are publicly available as part of the *Munich Quantum Toolkit* (MQT) at <https://github.com/cda-tum/mqt-qecc>. Such methods are an important step in providing fault-tolerant circuit constructions that can aid in near-term demonstrations of fault-tolerant quantum computing.

I. INTRODUCTION

Quantum bits and quantum operations suffer from unavoidable decoherence and noise. This leads to the fact that quantum error correction mechanisms need to be used to ensure that a quantum algorithm can be executed in a fault-tolerant manner to control the accumulation of errors. Error correcting codes leverage redundancy by encoding quantum information in logical qubits formed by entangled states of noisy, physical qubits. Consequently, it is important that universal operations can be carried out on the encoded information in a fault-tolerant way and that errors during the execution can be detected and corrected. Clearly, a crucial first step in a fault-tolerant circuit is the preparation of an encoded logical state.

To ensure that the logical state is initialized correctly—without containing too many errors—the preparation itself needs to be fault-tolerant. Intuitively, a requirement for fault-tolerant circuits is that errors on single qubits cannot uncontrollably “spread” to multiple qubits, for instance, through CNOT gates. For *Calderbank-Shor-Steane* (CSS) codes [1–3], one way of initializing

an encoded state fault-tolerantly is to prepare all physical qubits in $|0\rangle$ or $|+\rangle$ and perform one round of error correction—projecting the product state onto the logical code space [4]. For large code instances this overhead might be manageable, especially for QLDPC codes [5] and single-shot codes [6–9].

However, especially for smaller code instances that are relevant for near-to-midterm devices, this general procedure introduces a significant overhead in terms of circuit size since all stabilizer generators need to be measured multiple times. This makes near-term experimental realizations difficult.

An alternative scheme that tries to reduce the number of measurements is a non-deterministic protocol, based on post-selection [10–13]. Therein, initialization is performed in two steps:

1. Prepare the logical state using a non-fault-tolerant *state preparation circuit*.
2. Conduct specific measurements on the prepared states using a so-called *verification circuit* that detects if an error spreads through the circuit. If any of these measurements measure a -1 eigenvalue, the state is discarded, and the procedure is restarted.

While this and related techniques were successfully demonstrated in recent in experiments [11, 12, 14–19], there are clear drawbacks: First, these methods rely on

* tom.peham@tum.de

† ludwig.s.schmid@tum.de

‡ lucas.berent@tum.de

§ markus.mueller@fz-juelich.de

¶ robert.wille@tum.de

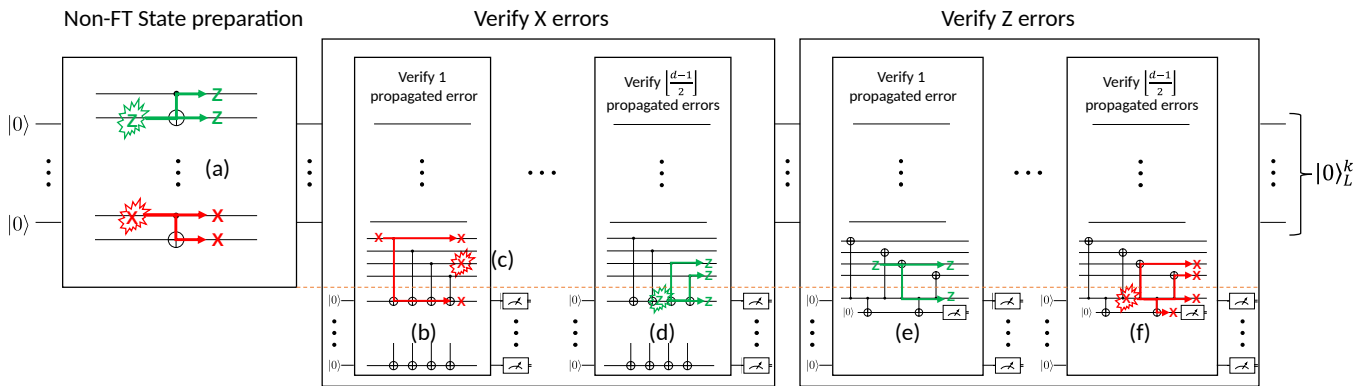


FIG. 1: Full non-deterministic fault-tolerant state preparation protocol for CSS codes. A sequence of stabilizer measurements follows a non-fault-tolerant state preparation circuit to check if any errors propagated through the circuit. The state is accepted if no measurement in the verification blocks indicates an error. **(a)** Errors in the non-fault-tolerant state preparation circuits propagate to higher-weight errors through CNOTs between data qubits. **(b)** If an error of at most weight i occurred in the state preparation circuit and propagated to a higher-weight error, measurements in the i th layer of the verification circuit detect this error. **(c)** Propagated errors are still detected by later layers of verification, even if further errors occur during a stabilizer measurement. **(d)** Z errors on the ancilla during the verification of X errors propagate to the data qubits. **(e)** If a Z error propagated through the non-FT state preparation circuit *or* the Z measurements of the previous verifications, it is later detected by flag fault-tolerant measurements. **(f)** Propagated X errors on the X measurement ancillas are detected by flag qubit measurements.

manual construction, which is tedious and becomes infeasible when scaling to larger codes where both the set of errors, and the possible verification measurements blow up. Moreover, as for the general scheme outlined above, there is no guarantee that these manually constructed circuits are gate- or depth-optimal. Finally, these constructions have mostly been explored for specific code instances for small distance 3 (or 2) codes [10, 12, 14, 20]. Even for code states beyond distance 3, constructions of non-deterministic circuits were derived manually for specific states [13] or codes [21, 22] and no general construction is provided. While such post-selection schemes do not scale well to large distances due to the exponentially decreasing acceptance rate, optimal circuit constructions might still be viable for moderately sized codes. In general, constructing a verification circuit that ensures that the overall scheme is fault-tolerant is highly non-trivial and depends on the code (and the logical state to prepare). The manual construction in existing works is thus not generally applicable. With ever-improving error rates on current devices, experimental demonstrations of higher distance codes might be possible with a verification-based scheme. For this, the construction needs to be generalized beyond distance 3, and algorithmic methods that can be applied to a broad range of codes must be developed.

In this work, we address these issues and propose *automated* methods for the synthesis of fault-tolerant state preparation circuits for *arbitrary* CSS codes. Our main contributions are as follows:

- We separate the synthesis problems for a state preparation and verification circuit and tackle each

one individually. We frame both problems as binary optimization problems and discuss their computational complexity to provide a motivation for the methods we employ.

- Based on that, we utilize satisfiability solving (SAT) techniques, which, through the use of highly optimized solving algorithms, have been shown to be successful in dealing with small instances of problems of corresponding computational complexity, see e.g., [23–29] for corresponding examples in the classical realm and, e.g., [30–34] for examples from the domain of quantum computing. This leads to *exact* solutions for the respective synthesis problem, which allows for synthesizing gate- or depth-*optimal* state preparation¹ and verification circuits.
- To address the scalability issues of SAT techniques, we also propose *heuristic* solutions for synthesizing state preparation and verification circuits. While they do not guarantee optimal solutions anymore, this will allow for a *scalable* automated synthesis. This eventually will allow for automated synthesis, as well as instances too large for SAT solvers.
- To use the proposed methods for synthesizing logical basis states for CSS codes with distances greater

¹ This approach can also be applied to general stabilizer state preparation circuit synthesis. This closes the gap on optimal constructions of these circuits from [35].

than 3, we propose a generalized non-deterministic fault-tolerant state preparation scheme that guarantees fault-tolerance by composing multiple verification circuits that each check for different sets of errors. The resulting scheme is summarized in Figure 1.

In short, our contributions can be viewed as providing (optimal) circuits for every sub-circuit depicted in Figure 1.

We use the proposed methods to synthesize non-deterministic fault-tolerant state preparation circuits for various CSS codes and provide numerical simulations of the constructed circuits under a circuit-level noise model using Stim [36] to investigate the success and the logical error rates. Comparison with the state-of-the-art reinforcement learning-based synthesis method from Ref. [20] shows that our methods are competitive—producing equally good or better circuits than the reinforcement learning agent. Numerical evaluations show that the proposed scheme does indeed generalize non-deterministic fault-tolerant state preparation beyond distance 3. Finally, all proposed methods are made publicly available in the form of open-source software as part of the *Munich Quantum Toolkit* (MQT [37]) at <https://github.com/cda-tum/mqt-qecc>.

The rest of this work is structured as follows. In Section II, we review notation, give fundamental notions from quantum coding, and define the notion of a fault-tolerant state preparation protocol. Section III describes the problem of synthesizing non-deterministic fault-tolerant state preparation circuits and positions our work in the context of existing approaches. In Section IV, we describe our optimal and heuristic synthesis methods for non-fault-tolerant state preparation for CSS codes. How to verify such circuits and make them fault-tolerant is then described in Section V, where we also discuss the computational complexity of this problem. Based on these building blocks, we then detail our generalized scheme for non-deterministic fault-tolerant state preparation in Section VI. Section VII shows the resulting circuit for our synthesis method for various CSS codes and numerically verifies that our proposed scheme prepares logical basis states of CSS codes in a fault-tolerant manner. Finally, Section VIII concludes this paper.

II. BACKGROUND

In this section, we review formal notation and discuss fundamental concepts that are needed throughout the work. Throughout we use $[i] = \{1, 2, \dots, i\} \subseteq \mathbb{Z}$.

A. Quantum Codes

An $[[n, k, d]]$ -stabilizer code [38] is defined by a stabilizer group S , which is an abelian subgroup of the n -qubit Pauli group \mathcal{P}_n . We require $-I \notin S$ s.t. the code is

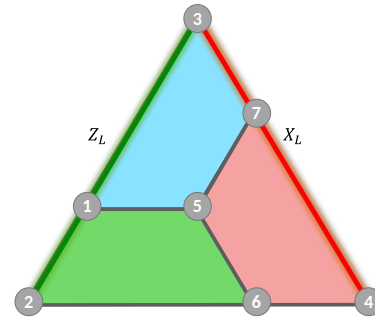


FIG. 2: Steane code. The qubits are placed on vertices, and X- and Z-stabilizer checks are associated with faces, acting on adjacent vertices.

non-trivial. The set of codewords, i.e., the k -dimensional codespace, is defined as the simultaneous $+1$ eigenspace of all elements in S . The generators of the stabilizer group $S = \langle g_1, g_2, \dots, g_m \rangle$ are called *checks*. They are used to infer whether a state is a codeword by measuring all m checks (using additional ancillas). The m measurement outcomes can be modeled as vector $s \in \mathbb{F}_2^m$ called the *syndrome*. If all syndrome bits are 0 (indicating a $+1$ measurement of the eigenvalue), the state is a codeword. Otherwise, the syndrome indicates which checks have failed and thus gives information about the approximate location of the error that occurred. The problem of finding a suitable recovery operation given the syndrome is called *decoding* and is a purely classical task.

A stabilizer code on n physical qubits with m checks encodes $k = n - m$ logical qubits. The *distance* d of the code is the minimum weight of an operator transforming one codeword into another.

A particularly important class of stabilizer codes are Calderbank-Shor-Steane (CSS) codes [1, 2], whose stabilizer generators g_i are either all X, or all Z. The corresponding sets are denoted S_X and S_Z , respectively. Note that since the support of X and Z type checks are disjoint, X and Z errors can be decoded independently.

Example II.1. The distance 3 color code, also called *Steane code*, is the smallest instance of a family of 2D planar color codes [39]. It can be visualized as depicted in Figure 2, where qubits are associated with vertices and stabilizer generators with faces. Hence, it is a $[[7, 1, 3]]$ CSS code defined by the stabilizer generators $S_X = \{X_1X_2X_5X_6, X_1X_3X_5X_7, X_4X_5X_6X_7\}$ and $S_Z = \{Z_1Z_2Z_5Z_7, Z_1Z_3Z_5Z_7, Z_4Z_5Z_6Z_7\}$. Logical operators are associated with the sides of the triangle. For example $X_L = X_3X_4X_7$ and $Z_L = Z_3Z_4Z_7$ would be minimal-weight logical X- and Z-operators (indicated by the red and green lines in Figure 2). Due to the symmetry of the X- and Z-stabilizers, $X_L = X_1X_2X_3$ and $Z_L = Z_3Z_4Z_7$ are also valid logical operators.

The stabilizer generators in S_X, S_Z can be mapped to

binary vectors that indicate the support of the respective Pauli operators, e.g., $XXII \in S_X$, $XXII \mapsto (1, 1, 0, 0) \in \mathbb{F}_2^n$. Hence, a CSS code can equivalently be defined as two binary matrices called *parity-check matrices*, $H_X \in \mathbb{F}_2^{r_X \times n}$, $H_Z \in \mathbb{F}_2^{r_Z \times n}$ whose rows are the binary vectors corresponding to the stabilizer generators. Since the X and Z type generators have to commute, the matrices have to fulfill the orthogonality condition $H_X H_Z^T = 0$.

Example II.2. The parity-check matrices of the Steane code are identical:

$$H_X = H_Z = \begin{pmatrix} 1 & 1 & & 1 & 1 \\ 1 & & 1 & 1 & \\ & & & 1 & 1 & 1 & 1 \end{pmatrix}. \quad (1)$$

B. Noise Model and Fault-Tolerance

We use a standard, depolarizing circuit-level noise model parameterized by the noise strength p , as discussed in more detail in Section VII.

The weight of an error E is defined as $wt(E) = \min_{E' \in E \cdot S} |supp(E')|$ i.e., as the minimal support of a stabilizer reduced error with respect to the stabilizer group S of the code. We say that an error *propagates* through a two-qubit gate if an error on one qubit before the gate leads to a two-qubit error after the two-qubit gate. We call an error in a circuit \mathcal{C} a *propagated error* if it propagates through any gate in \mathcal{C} .

There are slightly different meanings to the term *fault-tolerance* in the literature [40–42]. Intuitively, the definition we follow means that the uncontrolled spreading and accumulation of errors is avoided. More formally, we adhere to the following definition for a fault-tolerant state preparation protocol.

Definition II.3 (Fault-tolerant state preparation [43, 44]). A state preparation circuit is *strictly fault-tolerant* if for all $t \leq \lfloor \frac{d}{2} \rfloor$, any error of probability order t propagates to an error of weight at most t .

III. PROBLEM DEFINITION & MOTIVATION

In this section, we illustrate the problem of fault-tolerant state preparation with verification circuits and motivate the need for generalized automated approaches.

A. Considered Problem

Before starting any fault-tolerant quantum computation, the logical qubits have to be initialized in some logical state—usually a Pauli eigenstate of the quantum error correcting code used to encode the quantum information. These states are easily described for an $[[n, 1, d]]$ CSS code. The logical $|0\rangle_L$ state of the code is defined by the stabilizers of the code and the logical Z_L operator.

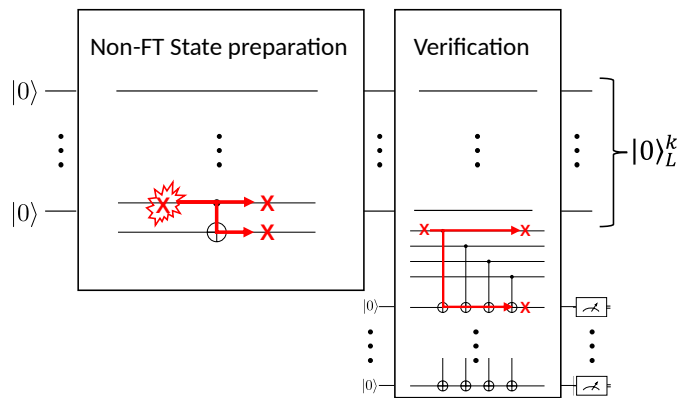


FIG. 3: Fault-tolerant Pauli-eigenstate preparation for stabilizer codes. A state is prepared with a non-fault-tolerant encoding circuit and the state is post-selected on a set of stabilizer measurements called the verification circuit. If one of these measurements flags, the state is discarded and the process restarted.

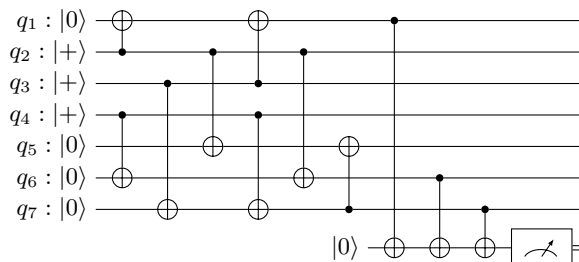


FIG. 4: Non-deterministic state preparation for the $|0\rangle_L$ of the Steane code from Ref. [10].

Similarly, the logical $|+\rangle$ state is defined by the stabilizers of the code and the logical X_L operator. The Pauli eigenstates of a general $[[n, k, d]]$ CSS code are defined analogously for corresponding pairs of logical operators $X_L^i, Z_L^i, i \in [k]$. For the remainder of this work, we will focus on the preparation of the logical $|0\rangle_L^k$ state, but the methods transfer directly to preparing the $|+\rangle^k$ state by swapping the roles of X and Z -stabilizers and operators and reversing the direction of every CNOT in the state preparation circuits.

A simple protocol for preparing Pauli eigenstates is to initialize all physical qubits in $|0\rangle$ and to project the product state onto the code space by measuring the stabilizers of the code. The logical Z_L^i operators are already stabilizers of the initial $|0\rangle^n$ and will still be a stabilizer of the projected state since the operators Z_L^i commute with the stabilizers of the code. These measurements are repeated $O(d)$ times to extract reliable syndrome information from the encoded state and to enable correction of any potential errors that have occurred using decoding [39, 45]. Additional CNOT overhead is incurred when using a flag-fault-tolerance scheme to measure the stabilizers [42]. This results in $(n - k) \cdot O(d)$ measurements in total in the worst case. For the Steane code, this proce-

dures requires $6 \cdot (4+2) \cdot 3 = 108$ CNOTs in the worst case, i.e., the 6 weight-4 stabilizer generators of the Steane code have to be measured 3 times—the distance of the Steane code—and each measurement requires another 2 CNOTs for the flags. For experimental realizations in near-term quantum computers, the error rate of these CNOTs will completely overshadow any error suppression theoretically guaranteed by the Steane code.

For this reason, recent experimental demonstrations of fault-tolerance have used a so-called *non-deterministic* scheme based on post-selection to produce high-fidelity logical states [11, 12, 14–19]. The idea of this approach is to prepare the logical state in a non-fault-tolerant manner and measure a set of stabilizers (which include logical operators) that detect any uncorrectable error caused by a correctable error propagating through the state preparation circuit. If one of these measurements is triggered, the state is discarded, and the whole process is restarted. The measurement circuit is referred to as the *verification circuit*. The protocol is sketched in Figure 3. The verification circuit depends on the specific state preparation circuit, as the errors that should be detected by the verification measurements are determined by the CNOT gate pattern in the state preparation circuit.

Example III.1. For the $|0\rangle_L$ state of the Steane code, the optimal non-deterministic preparation scheme uses 8 CNOTs for the preparation circuit and a single weight-three measurement of a logical Z_L operator [10] (cf. Figure 4) in the verification circuit. The only problematic stabilizer-inequivalent errors that can occur in the circuit are X_5X_7 and X_2X_6 . Both of these anti-commute with the measured $Z_L = Z_1Z_6Z_7$ operator and are thus detected in this verification measurement.

Ideally, the verification circuit only indicates an error if a propagated error occurs. Unfortunately, this is impossible in general. For example, any single qubit error on the measurement ancilla will trigger the verification measurements. The *acceptance rate* r_A of a non-deterministic preparation scheme is the probability that a state will be accepted, i.e., that no measurement in the verification circuit is triggered. This probability decreases exponentially with the number of measurements even when ignoring errors in the state preparation circuit itself: $p_A \leq (1 - p)^m$ where m is the number of measurements.

The goal of this work is to formulate a general algorithm that synthesizes a (near-)optimal circuit for each of these subcircuits for any $[[n, k, d]]$ CSS code.

B. Related Work

Recent work has tackled state preparation and verification circuit synthesis using reinforcement learning (RL) [20]. The biggest difference between our method and the RL approach is that we only focus on CSS codes, while the RL framework works for arbitrary stabilizer

codes. Furthermore, we ignore qubit connectivity constraints in this work while this aspect is accounted for in Ref. [20]. Lastly, the RL framework also provides a method for tackling the state preparation and verification circuit synthesis problem *simultaneously*, whereas we treat them separately. The downside of the RL-based approach is that it does not give any optimality guarantees. Since the code is a parameter in the training of the RL agent, the runtimes for synthesizing a single circuit are high, even for small codes.

Since CSS code state preparation circuits consist only of CNOT gates [46], the state preparation circuit synthesis problem is closely related to the synthesis of linear reversible circuits. This is a well-researched problem with known algorithms reaching the theoretical lower bound on circuit size and depth [47–49]. These algorithms provide systematic ways that are *asymptotically optimal*. These asymptotic analyses hide a significant constant overhead that we can’t ignore for the smaller system sizes we are mainly interested in. That is why our state preparation circuit synthesis approach is more closely related to greedy CNOT circuit synthesis methods as proposed in Ref. [50]. The most important difference between the considered problems and linear circuit synthesis is that we have more degrees of freedom. Although both problems can be framed in terms of matrix elimination over \mathbb{F}_2 , the matrices in our setting are not necessarily invertible. Therefore, many different circuits prepare the same state despite implementing different linear maps.

Another closely related problem is that of general Clifford and stabilizer state preparation circuit synthesis. For these, there are also optimal [34, 35, 51] and asymptotically optimal [49, 52–54] methods. Our SAT-based optimal state preparation circuit synthesis method especially is closely related to Ref. [34] and Ref. [35]. The optimal synthesis in Ref. [34] is focused only on the depth-optimal synthesis of Clifford circuits and does not provide an encoding to obtain (two-qubit) gate-optimal circuits. More importantly, as with the synthesis of linear circuits, there are more degrees of freedom than previous work does not take advantage of when focusing only on state preparation. The previous work on optimal stabilizer state preparation of Ref. [35] does not make use of this freedom either and does not guarantee the synthesis of a globally optimal circuit. Optimality is only guaranteed with respect to a specific stabilizer generator set. In the extreme case, Ref. [35] synthesizes a linear-sized circuit for the $|0\rangle^n$ state if a particularly unfortunate representation of its stabilizers is given as an input. For more complex states it is not clear which generating set for the state’s stabilizer group yields the best circuit. We address this specifically in Section IV.

IV. SYNTHESIS OF

STATE PREPARATION CIRCUITS

In this section, we present a method for creating logical basis states for any CSS code given the stabilizer generators of the code. We focus on creating $|0\rangle_L^k$ but the method works exactly the same for the $|+\rangle_L^k$ state by swapping the roles of X and Z stabilizer and changing directions of CNOTs. For the rest of this section, we consider an $[[n, k, d]]$ CSS code with m X stabilizer generators.

A. Problem Description and Complexity

Since the orthogonal complement of the X check matrix $H_X \in \mathbb{F}_2^{m \times n}$ is uniquely defined and coincides with the space spanned by the rows of H_Z and Z_L , $|0\rangle_L^k$ is uniquely fixed by the X stabilizers of the code alone. An important property of logical X or Z basis state preparation circuits of CSS codes is that they consist only of physical qubits initialized in the X or Z basis followed by a sequence of CNOTs. In fact, there is a one-to-one correspondence between such circuits and CSS codes [46]. If we have m qubits initialized in $|+\rangle$ and $n-m$ qubits in $|0\rangle$ then the product state of these qubits has m X -stabilizers and $n-m$ Z -stabilizers. Applying a CNOT to this state maps X -stabilizers to X -stabilizers and Z -stabilizers to Z -stabilizers. Therefore, any CNOT circuit applied to this initial product state does not change the number of X - or Z -stabilizers. Combined with the uniqueness of the orthogonal complement, this tells us that if the state obtained by applying a CNOT circuit to the initial product state is stabilized by the X -stabilizers of the code, it must necessarily also be stabilized by the Z -stabilizers and the logical Z -operators of the code and is, therefore, the $|0\rangle_L^k$ of the code. These properties simplify the considered problems significantly because, for state preparation, we only have to consider X stabilizers.

Any intermediate state during preparation is also a logical basis state of some CSS code with respective X checks H_X^a , where H_X^a denote the X -checks of the partial state after the first a CNOTs. If the $a+1$ st CNOT has control q_i and target q_j then H_X^{a+1} is obtained by adding column of H_X^a i onto column j of H_X^a . This comes from the fact that a Pauli X copies through the control of a CNOT. A CSS state preparation circuit \mathcal{C} on n qubits, therefore, implements an invertible matrix $M_{\mathcal{C}}$ over \mathbb{F}_2 converting H_X^0 to the final H_X .

Recall that the rows of H_X represent stabilizer generators for the X stabilizers of the given code. The choice of stabilizer generators is not unique in general. In particular, we can replace any two generators $\mathcal{X}_i, \mathcal{X}_j$ by equivalent generators $\mathcal{X}_i, \mathcal{X}_i \cdot \mathcal{X}_j$. We say that two check matrices H_X and H'_X are equivalent if $H_X = R \cdot H'_X$ for some invertible $\mathbb{Z}_2^{m \times m}$ matrix R .

The task of CSS state preparation circuit synthesis, then, is to find a CNOT circuit \mathcal{C} such that $H_X M_{\mathcal{C}} =$

$R \cdot [I \ 0]$ or, equivalently $H_X = R [I \ 0] M_{\mathcal{C}}^{-1}$. Here, we assumed without loss of generality that the qubits initialized in $|+\rangle$ are the first m qubits in the qubit ordering. The second formulation of the synthesis problem suggests that instead of constructing the circuit by successively adding CNOTs until we obtain H_X , we can start from H_X and apply CNOTs until we obtain the *reduced* check matrix $[A \ 0]$ where A is some rank $rn H_X \times rn H_X$ matrix.

Complexity-wise, generating optimal CNOT circuits is closely related to the minimum circuit size problem, which is unlikely to be proven to be in P or NP [55]. Therefore, it is unlikely to find a polynomial algorithm for state preparation circuit synthesis since it is simply a variant of that problem. In the following, we describe how to convert an instance of the state preparation circuit synthesis problem to a SAT formula and obtain gate- and depth-optimal preparation circuits. Since this reduction to SAT is not expected to scale due to the intractability of the SAT problem, we also provide a polynomial-time heuristic algorithm for this problem.

B. Optimal Approach

We would like to find an optimal preparation circuit whenever possible. Fewer CNOTs naturally lead to lower error rates in any circuit, and shallower circuits lead to faster execution time, which in turn leads to a decrease in idling errors. Therefore, we want to synthesize *gate-* and *depth-*optimal circuits.

Since the synthesis problem is formulated over \mathbb{F}_2 , SAT solvers [56] are a natural choice for this task. SAT solvers have previously been employed to synthesize general stabilizer circuits [34] and state preparation circuits in particular [35]. However, these approaches provide a solution only for a few qubits. We can improve upon these SAT encodings by taking advantage of the fact that we are dealing with CSS codes.

The idea behind the encoding is sketched in Figure 5. Essentially, the task is to symbolically encode Gaussian elimination over \mathbb{F}_2 . To this end, we first introduce *matrix variables* $\{x_{i,j}^t \mid 1 \leq i \leq m, 1 \leq j \leq n, 1 \leq t \leq t_{max} + 1\}$, where t_{max} is the given maximum number of elimination steps. The maximum number of elimination steps allows us to control how many CNOTs are applied at each step. Depending on the specific optimization task, we can use t_{max} to limit the total number of CNOTs or the depth of the circuit.

Initially, we assert that

$$\forall 1 \leq i \leq m. \forall 1 \leq j \leq n. x_{i,j}^1 = H_x[i, j].$$

For the reduced matrix, we assert the pseudo-boolean constraint

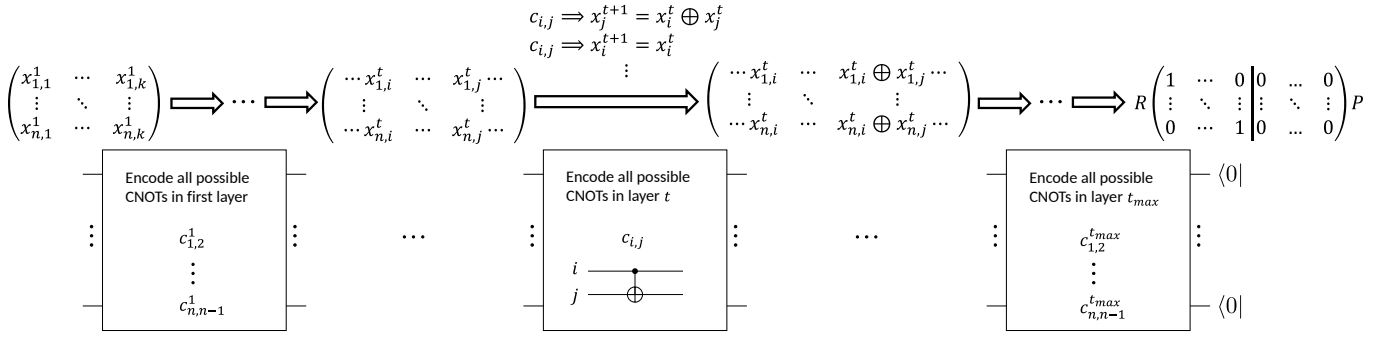


FIG. 5: Symbolic encoding for optimal state preparation circuit synthesis. The circuit is synthesized using at most t_{max} layers of CNOTs. All possible column additions on the symbolic check matrices are related via variables $c_{i,j}^t$, which encode all possible CNOTs in layer t . Starting from the target check matrix H_X these constraints encode all possible valid circuits that prepare the logical $|0\rangle_L^k$ state.

$$\left(\sum_{j=1}^n \left(\sum_{i=1}^{rnH_x^{t_{max}+1}} x_{i,j}^{t_{max}+1} \geq 1 \right) \right) = n.$$

In other words, the matrix must be reduced to a matrix $H_x^{t_{max}+1}$ with exactly $rnH_x^{t_{max}+1}$ columns with non-zero entries. This is equivalent to asserting that there exists an invertible matrix R and a permutation matrix P such that $RH_x^{t_{max}} = P [I_n \ 0]$. This constraint guarantees that the choice of stabilizer generators has no impact on the synthesized circuit's size.

Symbolic matrices in consecutive steps are obtained via column operations. Either a column is added onto another, or a column does not change. Therefore, we introduce two Boolean formulas

$$\begin{aligned} add(i, j, t) &= \forall 1 \leq k \leq m. x_{j,k}^{t+1} = x_{i,k}^t \oplus x_{j,k}^t \\ id(i, t) &= \forall 1 \leq k \leq m. x_{i,k}^{t+1} = x_{i,k}^t. \end{aligned}$$

No matter which of the two metrics we optimize for, obtaining the optimal state preparation circuit is achieved by solving the encoded formula for different values of t_{max} until two values t_1, t_2 are found such that

- The formula is unsatisfiable for $t_{max} = t_1$ and
- The formula is satisfiable for $t_{max} = t_2$.

The optimal solution is then the one obtained from the variable assignment to the satisfiable instance.

In the following, we will give the details of the encoding for synthesizing depth- and gate-optimal circuits.

Encoding for Depth-optimal Circuits

For synthesizing depth-optimal circuits, we interpret t_{max} as the maximal circuit depth. We then need only

to encode all possible layers of CNOTs at each reduction step. If the solver finds a satisfying assignment, we can extract the circuit directly from the variable assignment. If the solver shows no such assignment exists, we can incrementally vary t_{max} until a satisfying assignment is found.

We introduce *CNOT variables* $\{c_{i,j}^t \mid 1 \leq i \leq n, 1 \leq j \leq n, 1 \leq t \leq t_{max}+1\}$, which encode all possible CNOTs (or column additions) from control qubit (column) i to target qubit (column) j . These variables encode how the symbolic matrices at steps t and $t+1$ are related:

$$\begin{aligned} \forall 1 \leq t \leq t_{max}. \forall 1 \leq i \leq n. \\ \forall 1 \leq j \leq n, j \neq i. c_{i,j}^t \implies add(i, j, t). \end{aligned} \quad (2)$$

Additionally, any qubit can be involved in at most one CNOT at one timestep:

$$\forall 1 \leq t \leq t_{max}. \forall 1 \leq i \leq n. \left(\sum_{j=1}^n c_{i,j}^t + \sum_{j=1}^n c_{j,i}^t \right) \leq 1.$$

Lastly, if a qubit acts as a control qubit or is not involved in any CNOT, the corresponding column does not change:

$$\begin{aligned} \forall 1 \leq t \leq t_{max}. \forall 1 \leq i \leq n. \\ \left(\bigvee_{j=1}^n c_{i,j}^t \vee \left(\neg \bigwedge_{j=1}^n c_{j,i}^t \right) \right) \implies id(i, t). \end{aligned}$$

Encoding for Gate-optimal Circuits

Instead of encoding entire layers of CNOTs, symbolic matrices in consecutive elimination steps are related by only a single column addition. This can be achieved by augmenting the depth-optimal encoding with further

constraints prohibiting more than one CNOT occurring at every step as done in [35]. Alternatively, these additional constraints can be avoided by encoding all possible control and target combinations for each CNOT instead of every possible CNOT. By using a binary encoding for the control and target qubit indices, we require only $2n \lceil \log_2 n \rceil$ instead of $n(n-1)$ variables.

This can be achieved by introducing *bit-vector* variables $\{ctrl^t \mid 1 \leq t \leq t_{max}\}$ and $\{tar^t \mid 1 \leq t \leq t_{max}\}$ of size $\lceil \log_2 n \rceil$. We can then encode *CNOT constraints* relating the control and target variables:

$$c_{i,j}^t = ctrl = 1 \wedge tar = j.$$

With this, we can symbolically encode the column addition constraints using eq. (2).

Encoding the fact that a column does not change if the corresponding qubit is not the target of a CNOT is simpler in this setting:

$$\forall 0 \leq t < t_{max}. \forall 1 \leq i \leq n. tar^t \neq i \implies id(i, t).$$

Of course, a qubit cannot be both the target and control of a CNOT:

$$\forall 1 \leq t \leq t_{max}. ctrl^t \neq tar^t$$

Since the bit-vectors might take on values outside the allowed qubit range, we impose the following constraint:

$$\forall 1 \leq t \leq t_{max}. 1 \leq ctrl^t \leq n \wedge 1 \leq tar^t \leq n.$$

With these constraints encoded, we can try to obtain a solution using publicly available SMT solvers like Z3 [57].

C. Heuristic Approach

CNOT and stabilizer circuit synthesis have been well researched in the past, and various asymptotically optimal algorithms exist [47, 48, 54]. For small circuits, the constant overhead in these constructions leads to unacceptably large circuits.

In Ref. [50, 58], the authors propose a greedy path-finding-based method for synthesizing linear circuits. For an input Z_2 matrix H they define the cost functions

$$h_{\text{sum}}(H) = \sum_{i,j} H[i,j]$$

$$h_{\text{prod}}(H) = \sum_i \log \left(\sum_j H[i,j] \right).$$

The idea behind the second cost function is that it prioritizes columns that are almost completely zeroed. They

also propose to use the combined cost of H and H^{-1} to guide the search. Since the matrices, in our case, aren't invertible, this is not possible. Note that reducing the check matrix using such heuristics is a similar idea to the approach proposed in [43] where the ‘‘overlap’’ of stabilizers is used to reduce the CNOT count in state preparation circuits.

Such a greedy search strategy seems more promising for the smaller codes we focus on. Using the cost functions for a heuristic search will optimize for gates, but we also want to optimize for depth as much as possible. A simple heuristic is to construct the circuit layer by layer, always greedily choosing CNOTs that minimize the cost function until all qubits are involved in a gate or until no possible CNOT would decrease cost anymore.

An important point to note is that the greedy search can get stuck in local minima. In Ref. [50], an iteration limit is set before stopping the calculation. In our case, we can use the freedom to freely change the basis of the row-space to escape local minima when the synthesis algorithm is stuck. To this end, we can also greedily pick the row additions that remove the most ones². If even this approach fails, we can always fall back to doing Gaussian elimination on the rows of the matrix.

We make further use of this degree of freedom by preprocessing the matrix. The synthesized circuit will probably be quite deep if a matrix column has substantially more non-zero entries than other columns. This can be prevented by applying row operations that decrease the maximum column weight without decreasing the row weights.

V. SYNTHESIS OF VERIFICATION CIRCUITS

State preparation circuits like the ones we synthesize above are generally not fault-tolerant. The key idea to ensure fault-tolerance is to append a verification circuit to the preparation circuit that indicates whether an error has propagated in the circuit and post-selecting on the verification measurement outcomes. More specifically, a verification circuit is the circuit implementation of a specific set of stabilizer or logical operator measurements of the state such that any propagated error anticommutes with one of the verification measurements. An error anticommutes with a stabilizer measurement if their support overlaps on an *odd* number of qubits. Thus, the propagated errors of the state preparation circuit impose a parity constraint on the measurements used in the verification circuit.

In the following, we will describe the problem of synthesizing verification circuits in detail. In particular, we

² In principle, these reductions can be tried between every column operation to reduce the number of 1s in the matrix even faster. We have not observed a definite benefit of doing this as it sometimes actually leads to worse solutions.

describe the challenges that arise when generalizing verification circuit synthesis to codes with distances larger than 3. We show how the verification circuit synthesis problem can be broken down into synthesizing a sequence of verification circuits that verify a specific set of errors—significantly reducing the complexity of the problem.

To synthesize each subcircuit, we show how to encode the synthesis problem into a SAT formula. Iterative queries to a SAT solver can then again be used to find the gate- or ancilla-optimal sub-verification circuit. As with the optimal synthesis of state preparation circuits, there will be limits to scaling such an optimal synthesis method. We, therefore, also propose a scalable, greedy synthesis scheme.

A. Problem Description and Complexity

A simple way to synthesize a verification circuit is to measure all stabilizer generators, which might include many superfluous measurements. Note again that since we prepare logical basis states, the respective logical operators are also stabilizers of the state.

Define the i -fault set $\mathcal{E}_i(\mathcal{C})$ of a circuit \mathcal{C} as the set of propagated errors E with $wt(E) > i$ that are caused by the propagation of an error of probability order i . Computing this set itself takes $O(\#CNOTs^i)$ time and is therefore fixed-parameter tractable in the number of CNOTs. Since we will mainly look at small codes with a small number of CNOTs, computing this set is straightforward.

Let us continue to focus on the logical $|0\rangle_L^k$ state. Since we are looking at CSS codes, X and Z errors can be checked separately. Let us focus on verifying X errors for now. To check for X errors, any element of S_Z (including logical operators) can be measured in general. Searching for a minimally-sized set of measurements seems infeasible considering the size of this group. This is stated by the following theorem.

Theorem V.1. *Consider the following decision problem: Given an X fault set \mathcal{E} , Z stabilizer generators Z_1, \dots, Z_m and an integer k , is there a set of group elements $Z_{ver,1}, \dots, Z_{ver,t}$ such that $\sum_{i=1}^t wt(Z_{ver,i}) \leq k$ and for all $E \in \mathcal{E}$ there is a $Z_{ver,i}$ such that $E \cdot Z_{ver,i} = -E \cdot Z_{ver,i}$? This problem is NP-complete.*

Proof. The problem is clearly in NP, since given a certificate for an instance it is straightforward to verify that it is a valid solution. Furthermore, this is just a more general version of the Coset leader problem, which asks for a minimum-weight representative of the coset of some linear code. Computing such minimal-weight representatives is NP-complete [59] and is essentially a decoding problem. \square

Consider an $[[n, k, d]]$ code which protects against up to $t = \lfloor \frac{d-1}{2} \rfloor$ errors and a state preparation circuit \mathcal{C} for the $|0\rangle_L^k$ of this code. Generating a verification circuit for all

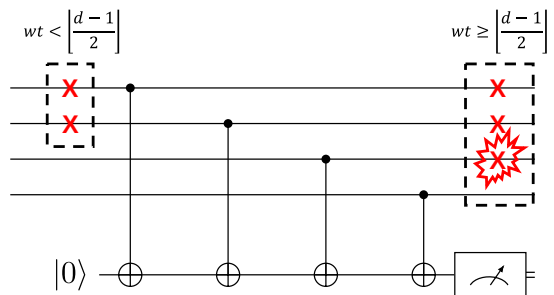


FIG. 6: A correctable error is (correctly) not detected by the verification circuit, but an error after the stabilizer measurement turns the error into an uncorrectable one. If this happens after the last measurement, which would detect this error, it goes by undetected.

X errors $\bigcup_{i=1}^{\lfloor \frac{d-1}{2} \rfloor} \mathcal{E}_i(\mathcal{C})$ does not ensure fault-tolerance in and of itself because errors can also occur in the verification circuit itself. We distinguish the following cases.

1. t errors occur in the non-fault-tolerant state preparation circuit and propagate to an *uncorrectable* error $E_C \in \mathcal{E}_t$ at the output.
2. $i < t$ errors occur in the non-fault-tolerant state preparation circuit and propagate to a *correctable* error $E_C \in \mathcal{E}_i$ at the output.
3. $i < t$ errors occur in the non-fault-tolerant state preparation circuit and propagate to an *uncorrectable* error $E_C \in \mathcal{E}_i$ at the output.

The first case will always be detected by the verification circuit, assuming that at most t errors occur in the entire state preparation circuit. In the second case, if another error E_{Ver} of weight $wt(E_{Ver}) = t - i$ occurs in the verification circuit, then it could be that $E_C \cdot E_{Ver} \notin \mathcal{E}_i$. If this error is not in the fault set $E_C \in \mathcal{E}_t$, then this error is equivalent to some non-propagated error. If it is in the fault set, however, it should be detected by some measurement in the verification circuit. But it could be that E_{Ver} happens after every measurement that would detect this combined error. Then, the state will not be discarded, and the fault-tolerance condition of Definition II.3 is violated (see also Figure 6).

In the third case, the verification circuit would detect the error, but if no more than $t - i$ measurements detect this error, then all these measurements could be flipped with at most $t - i$ independent errors. We say that the error is *masked*. The verification circuit would then indicate no error, and Definition II.3 is violated again (see Figure 7).

For distance 3 codes for which fault-tolerant verification circuit-based state preparation schemes exist, this is not much of an issue since in cases 2 and 3, the state preparation circuit would be error-free, i.e., $i = 0$. Every error in the verification circuit can introduce, at most, a

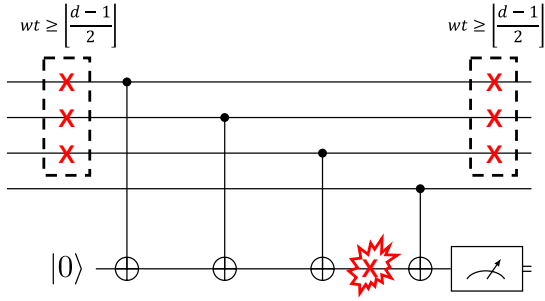


FIG. 7: An uncorrectable error would be detected by the verification circuit, but an error on the measurement ancilla flips the X parity, causing the measurement to falsely indicate no error (masked). If this happens after the last measurement that would detect this error, it goes by undetected.

weight 1 error on the data qubits, so case 2 is unproblematic. Even an error on a measurement ancilla will only trigger one of the verification measurements, leading to the state being discarded. For distance 3 codes, the verification circuit can, therefore, be treated as error-free without penalty.

Greater care must be put into synthesizing the verification circuit for larger distances. The case distinction above already suggests the solution. The verification circuit needs to detect not only uncorrectable propagated errors but correctable ones, too, as these might lead to a logical error together with additional errors in the rest of the circuit. Let Ver_i be a verification circuit for \mathcal{E}_i . We achieve fault-tolerance against one type of error with the verification circuit

$$Ver = Ver_t \circ Ver_{t-1} \circ \dots \circ Ver_1, \quad (3)$$

where \circ denotes circuit composition.

As before, if any measurement in this circuit indicates an error, the state is discarded, and the process is started anew. This ensures fault-tolerance by the following reasoning:

Let E be a propagated error with $wt(E) > i$ caused by $i < t$ errors in the state preparation circuit. E will be detected by $Ver_{wt} \circ Ver_{i+1} \circ Ver_i$. Masking E will, therefore, require at least another $wt(E) - i$ errors on the measurement ancillae since in any intermediate verification circuit, at least one measurement will detect E . If E is masked, a total of $i + (wt(E) - i) = wt(E)$ independent errors have to have occurred before $Ver_{wt(E)+1}$. The weight of the error on the data qubits can be increased by another $t - wt(E)$ independent errors. But the maximal weight error achievable is then $t - wt(E) + wt(E) = t$ which is correctable.

Errors on the data qubits can also happen somewhere in $Ver_{w(E)} \circ Ver_{i+1} \circ Ver_i$. In fact, a two-qubit error E' in one of the CNOTs of Ver_j might both increase the error weight and mask E at the same time. But that

just offsets detection because now $E \cdot E'$ is detected by $Ver_{w(E)+1} \circ Ver_{wt(E)} \circ Ver_{j+1}$. Assuming that $E \cdot E'$ is masked without increasing weight, the number of independent errors that occurred before $Ver_{wt(E)+2}$ is

$$\underbrace{i}_{\text{state prep}} + \underbrace{(j-1-i)}_{\text{masking}} + \underbrace{1}_{Ver_j} + \underbrace{((wt(E)+1) - (j+1))}_{\text{masking}}$$

which again comes out to $wt(E)$. Similar reasoning as above tells us that in this case, further independent single errors will not result in an uncorrectable error. This argument can be repeatedly applied if further two-qubit errors occur in the verification circuit. Therefore, Ver ensures fault-tolerance for t errors.

The layered construction of the verification circuit simplifies the problem of verification circuit synthesis significantly. Instead of synthesizing the verification circuit wholesale, every layer can be constructed individually. Every \mathcal{E}_i gives rise to a new instance of the verification circuit synthesis problem. For every \mathcal{E}_i we have to find a set of stabilizer measurements such that every error in \mathcal{E}_i commutes with at least one of these measurements.

This layered approach significantly simplifies reasoning about verification circuit constructions by breaking the synthesis down into the synthesis of smaller sub-problems. This, however, potentially comes at the price of the “global” optimality of the full circuit. Since the different fault-sets of the preparation and verification circuits are not necessarily independent, synthesizing the verification circuits separately might lead to certain errors redundantly being verified multiple times. Hence, in this work, we only consider optimal constructions for each subcircuit.

Next, we will show optimal and heuristic algorithms to tackle these individual synthesis problems.

B. Optimal Approach

We can frame the optimal verification circuit synthesis problem again as a SAT problem with the following inputs:

- \mathcal{C} : a state-preparation circuit over n_q qubits.
- $H_X \in \mathbb{Z}_2^{m \times n}$: matrix representation of m X stabilizer generators of C .
- $H_Z \in \mathbb{Z}_2^{(n-m) \times n}$: matrix representation of $n - m$ Z stabilizer generators of C .
- n_{anc} : maximum number of ancillas (measurements) used in the verification circuit.
- n_{CNOT} : Maximum number of CNOTs used in the verification circuit.

Let $\mathcal{E}(C)$ denote the set of uncorrectable errors arising from propagating up to $\lfloor \frac{d}{2} \rfloor$ independent X errors and let E_i denote the \mathbb{Z}_2^n representation of the i -th error in $\mathcal{E}(C)$.

The Z -generators $\mathcal{Z} = \{Z_1, \dots, Z_{n-m}\}$ form a basis of the Z -stabilizers, so we can express any verification circuit as a set of \mathbb{Z}_2^{n-m} vectors indicating the contributing generators. We introduce the Boolean variables

$$\{v_s^i \mid 1 \leq i \leq n_{anc}, 1 \leq s \leq n - m\}.$$

An assignment to these variables denotes measurement s as a linear combination of the $n - m$ Z -stabilizer generators.

The j -th entry of the i -th measurement can be symbolically computed via

$$meas_j^i = \bigoplus_{s=1}^{n-m} v_s^i \wedge H_Z[s, j].$$

Assuming that H_Z is sparse it is not efficient to convert the Z stabilizers to Boolean constants and then perform these nested XOR operations. Since $a \oplus 0 = a, a \wedge 1 = a$ and $a \wedge 0 = 0$, we can simplify the computation by evaluating constants in Boolean functions before encoding the SMT formula. Such simplifications have been shown to lead to dramatic speedups in SMT solving [33].

Next, we need to ensure that every error is detected. Recall that an error is detected if it overlaps with a measurement on an odd number of qubits. Instead of computing the overlap on all qubits, we can again simplify this constraint by only considering qubits where an error actually has support. This way we can encode this parity constraint as a pseudo-boolean constraint. Every error E_k gives rise to a function

$$detected^{(k,i)} = \left(\sum_{j \in \text{supp}(E_k)} meas_j^i = 1 \right).$$

Every error needs to be detected by at least one measurement so we impose

$$\bigwedge_{k=1}^{|\mathcal{E}(C)|} \left(\bigvee_{i=1}^{n_{anc}} detected^{(k,i)} \right).$$

We can furthermore restrict the overall number of CNOTs used in the verification circuit with the pseudo-boolean constraint:

$$\left(\sum_{i=1}^{n_{anc}} \sum_{j=1}^{n_q} meas_j^i \right) \leq n_{CNOT}.$$

Since this encoding takes the maximal number of ancillae and the maximal number of CNOTs as parameters, we can iterate on both parameters to find either ancilla- or gate-optimal verification circuits.

C. Heuristic Approach

A part of the difficulty of computing verification circuits is the size of the stabilizer group from which measurements need to be chosen. Instead of searching through the entire group, we can try to find a suitably large set of *candidate* measurements and try to find a good subset as a verification circuit. Indeed if more than one measurement is required to verify a given fault-set the main difficulty is to identify a small set of verification measurements. The requirement of finding a small set of measurements such that every error is detected by at least one measurement is similar to the SET COVER [60] problem. The difference in our setting is that the number of potential stabilizers (covering sets) might be very large. We therefore consider this modified version of SET COVER:

- Given a set U , a collection of subsets P and an integer t .
- Define $P_1 = P$ and $P_k = P_{k-1} \cup \{A \Delta B \mid A, B \in P_{k-1}\}$, where Δ denotes the *symmetric difference* of sets.
- Find $Cov \subseteq \bigcup_{i=1}^t P_k \subseteq \mathcal{P}(U)$ such that $\bigcup_{A \in Cov} A = U$ and Cov is of minimal size.

By identifying $S \in \mathcal{Z}$ with the set $E(S) = \{F \in \mathcal{E}(C) \mid S \cdot F = -F \cdot S\}$, for two stabilizers $S_1, S_2 \in \mathcal{Z}$ we have $E(S_1 \cdot S_2) = E(S_1) \Delta E(S_2)$, i.e., any error that anticommutes with both S_1 and S_2 will not anticommute with their product and therefore will not be detected by the respective measurement. With this translation, we can phrase an instance of verification circuit synthesis as an instance of the above-defined modified SET COVER problem.

The straight-forward greedy algorithm for SET COVER approximates the optimum quite well [61], so we can use a similar strategy for synthesizing a verification circuit. The idea is to start with the stabilizer generators and iteratively expand the set of candidate measurements by building products of stabilizers in the candidate set. In each iteration, we can try to find a small set of stabilizers such that all errors are detected. If increasing the candidate set does not lead to a verification circuit with fewer stabilizer measurements, we stop. Alternatively, if the size of the candidate set reaches some pre-defined limit, we can take the best solution found until this point and terminate. This greedy algorithm is formalized in [Algorithm 1](#)

Let us make two remarks about the implementation of [Algorithm 1](#):

- When solving SET COVER in lines 2 and 4 there might be multiple choices for every greedy choice of set. In this case, we preferably pick the set that corresponds to lower-weight stabilizers.

Algorithm 1: Heuristic Verification Circuit

Data: Set of errors \mathcal{E} , Z -stabilizer generators \mathcal{Z} , maximal candidate set size c_{max}

Result: Set of stabilizer measurements \mathcal{Z}_{ver} that detect \mathcal{E}

```

1  $P \leftarrow \{E(S, \mathcal{E}) \mid S \in \mathcal{Z}\};$ 
2  $Cov \leftarrow$  greedy solution to SET COVER( $P, E(S)$ );
3 while  $|P| \leq c_{max}$  do
4    $Cov_{new} \leftarrow$  greedy solution to SET COVER( $P, E(S)$ );
5   if  $|Cov_{new}| = Cov$  then
6     break;
7    $P \leftarrow P \cup \{A \Delta B \mid A, B \in P\};$ 
8    $Cov \leftarrow Cov_{new};$ 
9  $\mathcal{Z}_{ver} \leftarrow$  Stabilizers corresponding to  $Cov$ ;
10 return  $\mathcal{Z}_{ver}$ ;
```

- Extracting the stabilizers from the set cover in line 11 can be done efficiently by maintaining a map from sets to stabilizer products.

In general, the candidate set can become large very quickly as, in the worst case it doubles in size during every iteration of the while-loop. For this reason, [Algorithm 1](#) takes the parameter c_{max} to limit the growth of this set.

By design, [Algorithm 1](#) only aims at minimizing the number of measurements in the verification circuit and not the weight of those measurements. This approach is appropriate when trying to minimize the overall number of measurements but might result in a few high-weight stabilizer measurements. This problem can be somewhat mitigated by completely removing high-weight measurements from the set of measurement candidates. However, a few high-weight measurements could actually be less costly in terms of the number of CNOTs than many low-weight measurements. The preferred choice might, for example, depend on the noise characteristics of the respective hardware under consideration.

After an appropriate set of stabilizers has been found using [Algorithm 1](#), we can try to minimize the weight of these stabilizers. If there are stabilizers $\mathcal{Z}_{red} = \{S \in \langle \mathcal{Z} \rangle \mid \mathcal{E}(S, E) = \emptyset\}$, i.e., stabilizers that commute with all errors, then they form a group $\langle \mathcal{Z}_{red} \rangle$. Given a verification stabilizer S_{ver} and any $S_{red} \in \langle \mathcal{Z}_{red} \rangle$ we can replace S_{ver} by $S_{ver} \cdot S_{red}$ in the verification circuit without changing which errors are detected. Another way to phrase this is to say that replacing S_{ver} by any element in the coset $S_{ver} \cdot \langle \mathcal{Z}_{red} \rangle$ yields a valid verification circuit. Give the measurements output by [Algorithm 1](#) we can therefore try to find the minimal representatives in their respective cosets, i.e., the so-called coset leader. As noted above, computing the minimal-weight representatives of these cosets is NP-hard [59]. Apart from constructing the standard array (i.e., listing all coset elements), there are methods using techniques from computer algebra [62, 63], which still require exponential memory in the worst case [64]. As a post-processing step,

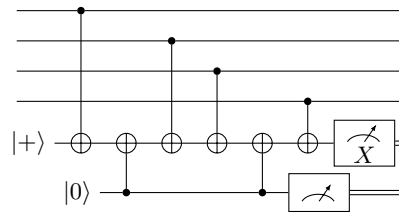


FIG. 8: Flag fault-tolerant measurement of a weight-4 stabilizer [42]

we can apply a heuristic search for the coset leaders of our verification stabilizers. One can also relegate this step to an SMT solver. For small codes, this can be expected to be efficient even if the global optimal verification circuit cannot be computed with the optimal method in an adequate amount of time.

VI. FULLY FAULT-TOLERANT NON-DETERMINISTIC STATE PREPARATION

Until now, we have only considered verification circuits for one type of error, i.e., X errors in preparing the $|0\rangle_L^k$. But even though Z errors cannot cause a logical error on $|0\rangle_L^k$, propagating Z errors through the state preparation circuit still violates the fault-tolerant requirement of [Definition II.3](#). A straightforward fix to this is generating verification circuits Ver_X and Ver_Z according to [Section V](#) that check for X and Z errors respectively and combine them to the verification circuit $Ver = Ver_X \circ Ver_Z$. This does not work however, because X (Z) errors on one of the ancillae in Ver_X (Ver_Z) can propagate to a higher weight error on the data qubits. This is commonly referred to as a *hook error* [45].

Unfortunately, there is no way to fix this predicament by introducing further stabilizer measurements since the new measurements can themselves be faulty. Instead, the hook errors have to be checked for specifically. Flag fault-tolerant stabilizer measurements have been introduced to solve this exact problem [42, 65]. The idea is to add further “flag” ancillae that interact with the stabilizer measurement ancilla via a pair of CNOTs that—in the absence of errors—act as identity. However, if any error occurs on the measurement ancilla, it propagates to at least one of the flags and is detected. See [Figure 8](#) for an example of a weight 4 flag fault-tolerant measurement.

Flag fault-tolerance was conceived as a way to give decoders additional information to account for hook errors, which can lead to complicated decision trees for decoders depending on the exact pattern of flags that measure an error. We require no such finesse and opt to include the flag measurements as further measurements upon which we post-select. If any flag is measured in -1 , this indicates that an error was propagated from an ancilla to the data, and we discard the state.

Not all stabilizers have to be measured flag fault-

tolerantly. If we measure Ver_X first, we can account for any hook errors introduced by this circuit by adapting the measurements for Ver_Z . Only Ver_Z , then, has to be measured using flags. Depending on the code and state preparation circuit, reversing the order of verification circuits might be better in terms of CNOTs. Still, only the second verification circuit has to be flag fault-tolerant. With this flag-fault-tolerant measurement scheme for the second error type, we arrive at the proposed scheme sketched in [Figure 1](#).

At this point, we have to revisit the issue of optimal circuits for the verification circuit synthesis. The introduction of flag-fault-tolerant measurements complicates the gate-optimality of the verification measurements even for the individual fault sets. First, no generally optimal flag scheme is known [42, 65]. Secondly, there is also a trade-off between the size weight of the measured stabilizers and the size of the corresponding flag circuit. It might, therefore, be better to measure more low-weight stabilizers with low flag overhead instead of high-weight stabilizers with high flag overhead. Note that depending on the minimum-weight stabilizer generators of the given code, the use of flag-qubits can not always be avoided.

We leave the problem of solving this global optimization problem for future work. In this work, we focus on providing locally optimal state preparation and verification circuits without considering flag overhead.

VII. NUMERICAL EVALUATIONS

The implementation of the methods presented in this work is publicly available as part of the Munich Quantum Toolkit [37] at <https://github.com/cda-tum/mqt-qecc>. To evaluate the efficacy of the proposed methods, we have synthesized state preparation circuits for various CSS codes.

A. Circuit Construction

First, we focus on the investigation of pure circuit metrics. We generate non-deterministic fault-tolerant state preparation circuits for various CSS codes using both the SMT and heuristic methods proposed in [Section IV](#) and [Section V](#). This allows us to investigate the scalability of the exact approach as well as how close the heuristic approach is to the optimum. In addition to that, we also compare the results to solutions generated in [20] (as reviewed in [Section III B](#), a synthesizer based on reinforcement learning). Note that, on our machine, the RL agent does not manage to find state preparation circuits within 24 hours for codes with 12 or more physical qubits. In this case, we used the best circuit from the examples provided at <https://github.com/remmyzen/rfftqc>.

[Table I](#) and [Table II](#) provide a summary of the circuits

obtained for both gate- and depth-optimization³, respectively. The tables list the CNOT count and depth of the non-fault-tolerant state preparation and verification circuits obtained from the proposed optimal and heuristic methods as well as the RL agent. More precisely, the first two columns denote the code and the prepared logical state, while the remaining columns denote the metrics of the obtained state preparation and verification circuits. SAT denotes the exact results, heuristic the heuristic, and RL the solution obtained by [20].

For this comparison, we focussed on verification circuits only for the primary type of error (X errors for the preparation of $|0\rangle_L^k$ and Z errors for the preparation of $|+\rangle_L^k$).

These results show that for small codes, all methods produce very similar results. However, for the cases where all methods produce the same circuit, the optimal method also yields an automatic proof that the obtained circuit is, in fact, gate- or depth-optimal. For larger codes, both the optimal synthesis method and the RL method fail to yield a result within the 24-hour timeout. For the optimal synthesis methods specifically, the state preparation times out—the verification circuit synthesis scales much more favorably. Moreover, the proposed approach clearly outperforms the RL synthesizer.

For codes with more qubits (≥ 17), the heuristic state preparation circuit starts to outperform the RL synthesis both in terms of CNOT count and circuit depth. For larger codes, the SMT and RL synthesis fail (indicated by “–” in the table) to produce any state preparation circuit within 24 hours. The heuristic synthesis, however, generates all circuits in under one second. Even in cases where the SMT solver cannot find an optimal state preparation circuit, it is still possible to find the optimal verification circuit (for the state preparation circuit generated by the heuristic synthesis). From these tables, we can conclude that synthesizing state preparation circuits using our greedy heuristic approach in combination with the optimal verification circuit synthesis can produce competitive non-deterministic fault-tolerant state preparation circuits even for moderately-sized codes.

We use our methods to generate fully fault-tolerant circuits as described in [Section VI](#). We again give the optimal synthesis method a 24-hour timeout. If the solver does not manage to find a solution in this timeframe we use the heuristic method instead. [Table III](#) shows circuit metrics for gate-optimized circuits found using this approach. These circuits are partially listed in [Appendix A](#). All circuits listed in [Table III](#) are also publicly available as part of the open-source implementation. For an example of a fault-tolerant state preparation of $|0\rangle_L$ for a distance 5 code, consider [Figure 15](#). There, we see that

³ Note that the RL method is not optimised to minimize circuit depth, but produces for various attempts different circuits of varying depth. Here, we report the instance, which for minimal obtained CNOT count has lowest depth.

TABLE I: Circuit metrics for fault-tolerant state preparation circuits obtained using our optimal (SAT) and heuristic approach when optimizing for CNOT count, and comparison with the recently proposed RL method [20]

Code	State	State Preparation Circuit						Verification Circuit					
		#CNOTs			Depth			#CNOTs			#Measurements		
		SAT	Heuristic	RL	SAT	Heuristic	RL	SAT	Heuristic	RL	SAT	Heuristic	RL
[[15, 1, 3]] Reed-Muller (tetrahedral) code [66]	$ 0\rangle_L$	22	22	22	4	4	7	3	3	3	1	1	1
	$ +\rangle_L$	23	23	24	5	5	6	7	7	7	1	1	1
[[9, 1, 3]] Shor Code [67]	$ 0\rangle_L$	8	8	8	5	6	5	3	3	3	1	1	1
	$ +\rangle_L$	6	6	6	2	2	2	0	0	0	0	0	0
[[9, 1, 3]] Rotated Surface Code [68]	$ 0\rangle_L$	8	8	8	5	6	3	3	4	3	1	1	1
[[15, 7, 3]] Hamming Code [69]	$ 0\rangle_L$	-	22	-	-	12	-	6*	7	-	2	2	-
[[17, 1, 5]] 2D Color Code [70]	$ 0\rangle_L$	-	23	25	-	11	7	29*	32	-	6*	5	-
[[19, 1, 5]] 2D Color Code [70]	$ 0\rangle_L$	-	27	-	-	8	-	33*	38	-	6*	6	-
[[25, 1, 5]] Rotated Surface Code [68]	$ 0\rangle_L$	-	28	-	-	13	-	34*	34	-	5*	5	-

Entries marked with "*" denote circuits where the optimal verification circuit was generated for the heuristic state preparation circuit.
 Entries with a "-" denote instances where the respective method failed to provide a circuit within the timeframe of 24h.
 Entries in bold denote instances where the obtained circuits using our methods yields improved metrics.

TABLE II: Circuit metrics for fault-tolerant state preparation circuits obtained using our optimal (SAT) and heuristic approach when optimizing for circuit depth, and comparison with the recently proposed RL method [20]

Code	State	State Preparation Circuit						Verification Circuit					
		#CNOTs			Depth			#CNOTs			#Measurements		
		SAT	Heuristic	RL	SAT	Heuristic	RL	SAT	Heuristic	RL	SAT	Heuristic	RL
[[15, 1, 3]] Reed-Muller (tetrahedral) code [66]	$ 0\rangle_L$	22	22	22	4	4	7	3	7	3	1	2	1
	$ +\rangle_L$	23	23	24	5	5	6	7	7	7	1	1	1
[[9, 1, 3]] Shor Code [67]	$ 0\rangle_L$	8	9	8	3	3	5	3	5	3	1	2	1
	$ +\rangle_L$	6	6	6	2	2	2	0	0	0	0	0	0
[[9, 1, 3]] Rotated Surface Code [68]	$ 0\rangle_L$	8	8	8	3	3	3	3	4	3	1	1	1
[[15, 7, 3]] Hamming Code [69]	$ 0\rangle_L$	23	22	-	4	4	-	8*	10	-	2*	2	-
[[17, 1, 5]] 2D Color Code [70]	$ 0\rangle_L$	-	23	25	-	4	7	28*	31	-	6*	5	-
[[19, 1, 5]] 2D Color Code [70]	$ 0\rangle_L$	-	27	-	-	4	-	33*	43	-	5*	6	-
[[25, 1, 5]] Rotated Surface Code [68]	$ 0\rangle_L$	-	28	-	-	4	-	35*	38	-	4*	5	-

Entries marked with "*" denote circuits where the optimal verification circuit was generated for the heuristic state preparation circuit.
 Entries with a "-" denote instances where the respective method failed to provide a circuit within the timeframe of 24h.
 Entries in bold denote instances where the obtained circuits using our methods yields improved metrics.

the verification circuit accounts for a large part of the entire circuit compared to the non-fault-tolerant state preparation subcircuit.

B. Logical Error Rate Simulation

To show that the synthesized circuits indeed yield the expected logical error rates, we have simulated them using the open-source stabilizer simulator Stim [36] under a standard circuit-level depolarizing noise model. That is, noisy gates are modeled as ideal gates followed by a depolarizing noise channel parameterized by an error probability p . To model noisier two-qubit gates, the single-qubit- and two-qubit-depolarizing channels are parameterized by different probabilities p_{sqg} and p_{tqg} , respectively:

$$\epsilon_1(\rho) = (1 - p_{sqg})\rho + \frac{p_{sqg}}{3}(X\rho X + Y\rho Y + Z\rho Z)$$

$$\epsilon_2(\rho) = (1 - p_{tqg})\rho + \frac{p_{tqg}}{15} \sum_{E \in \mathcal{E}} E\rho E,$$

where $\mathcal{E} = \{P_1 \otimes P_2 \mid P_1, P_2 \in \{I, X, Y, Z\}\} \setminus \{I \otimes I\}$. In addition, there is a probability of p_{sqg} that a qubit

will erroneously be initialized in the -1 eigenstate of the respective basis and measurements have a p_{sqg} probability of being flipped. If a qubit is idle during one layer of CNOTs, it is also subject to single-qubit depolarizing "idling" noise. What constitutes a layer of CNOTs depends on the computational model. We consider the two extreme cases: either all parallel CNOTs are executed in one layer, or only one CNOT can be performed in each layer. For our simulations we set $p_{sqg} = \frac{2}{3}p_{tqg}$.

Simulation runs for which any of the verification measurements indicate an error are discarded. For the remaining states, we calculate the logical error rate by measuring all data qubits in the Z basis, performing one round of ideal syndrome extraction and correction using a lookup-table decoder. A logical error is registered when the corrected classical bitstring anticommutes with any of the Z operators of the code. For each physical error rate p , we sample until we have collected 500 logical errors. For our simulations, this ensures that the uncertainties for the logical error rates are below 2% for all runs.

The results of the simulations with parallel gates are shown in Figure 9. For all codes, we find that the observed error suppression is in agreement with the ex-

TABLE III: Circuit metrics for the best circuits found using the proposed methods for the generalized non-deterministic fault-tolerant state preparation scheme.

Code	State	#Qubits	#CNOTs	Depth
[[15, 1, 3]] Reed-Muller (tetrahedral) code [66]	$ 0\rangle_L$	16	25	8
	$ +\rangle_L$	15	23	5
[[9, 1, 3]] Rotated Surface Code [68]	$ 0\rangle_L$	10	11	8
	$ 0\rangle_L^{\frac{1}{2}}$	15	30	17
[12, 2, 4] “Carbon” code [18]	$ 0\rangle_L^{\frac{1}{4}}$	17	28	13
[15, 7, 3] Hamming Code [69]	$ 0\rangle_L$	28	65	26
[17, 1, 5] 2D Color Code [70]	$ 0\rangle_L$	40	114	30
[19, 1, 5] 2D Color Code [70]	$ 0\rangle_L$	41	103	27

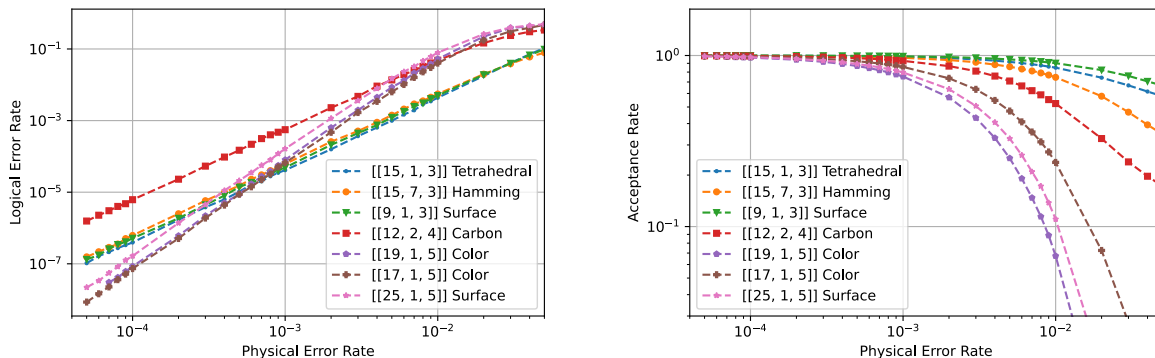


FIG. 9: Logical error rate and acceptance rate for non-deterministic fault-tolerant state preparation circuits for the logical $|0\rangle_L^k$ state constructed with our methods for various $d = 3$ and $d = 5$ CSS codes under circuit-level depolarizing noise using a LUT decoder.

pected error rate relative to the distance d of the code ⁴. All simulated distance $d = 3$ codes exhibit a $p_L \sim O(p^2)$ scaling of the logical error rate, whereas the distance $d = 5$ codes exhibit $p_L \sim O(p^3)$ scaling. This shows that the circuits produced with our methods indeed generalize the post-selection scheme previously known for distance $d = 3$ codes to higher distances $d > 3$. Moreover, though the acceptance rates for larger codes are drastically worse for high physical error rates, this difference becomes negligible for physical error rates $p < 2 \cdot 10^{-4}$, where all verification circuits accept the prepared state in $> 90\%$ of the cases.

To illustrate the performance of distance $d = 5$ state preparation more clearly, we compare the optimized state preparation circuits with a “naive” (canonical) verification circuits, where all stabilizers are measured twice. In addition, to visualize the impact of gate parallelism, we simulate the circuits with parallel gates and sequential

gates. The respective results can be seen in Figure 10 and Figure 11. These results show that optimizing the proposed generalized non-deterministic fault-tolerant state preparation scheme brings little to no benefit for higher distances if gates can be executed in parallel. This is due to the fact that even though the CNOT count of the optimized circuit is significantly lower, the depth of the optimized circuit is about as high as the depth of the naive verification circuit. The acceptance rate of the optimized circuit naturally scales much better. However, with physical error rates below $5 \cdot 10^{-4}$ where the larger codes exhibit better physical error rates, the difference in acceptance rate is negligible.

The improvement of the optimized circuits is drastic when all CNOTs have to be executed sequentially. In this case, the optimized scheme outperforms the naive one by orders of magnitude in logical error and acceptance rates.

These results show that optimized state preparation schemes are suited for quantum computing platforms with a lower degree of parallelism. For architectures like neutral atoms [17, 71] where two-qubit gates can be performed globally, the difference is less stark, assuming idling errors are manageable. For these systems, alternative schemes with a high degree of parallelism, like in the preparation of the Golay code [43], could be exploited.

⁴ Note that, as pointed out e.g. in Ref. [18], if one operates the quantum circuit for the [12, 2, 4] carbon code in an error detecting regime, i.e. each run with any error (on data qubits) triggering a stabilizer is discarded, all two-error events will be sorted out, and one obtains a $\sim p^3$ scaling for the logical error rate. In our simulations we focus only on single errors in the preparation of the carbon code states.

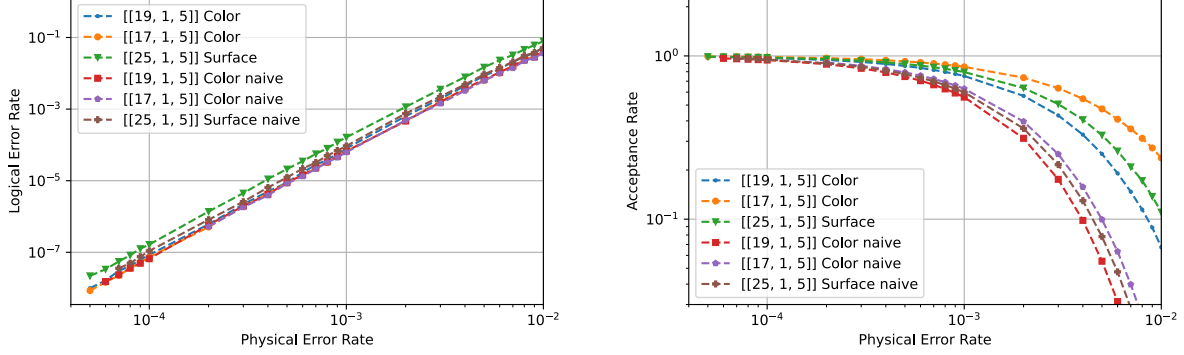


FIG. 10: Logical error rate and acceptance rate for non-deterministic fault-tolerant state preparation circuits for the logical $|0\rangle_L$ state constructed with our methods for 2D color and surface codes with $d = 5$ under circuit-level depolarizing noise with *parallel* gate execution using a LUT decoder.

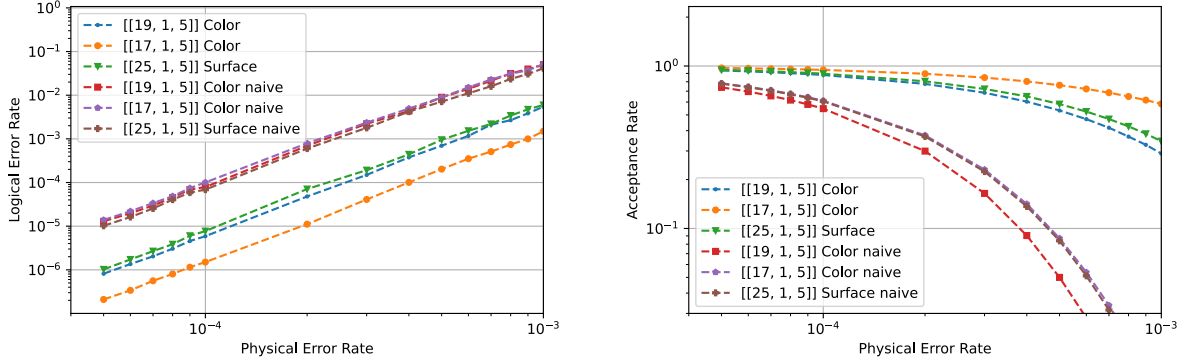


FIG. 11: Logical error rate and acceptance rate for non-deterministic fault-tolerant state preparation circuits for the logical $|0\rangle_L$ state constructed with our methods for 2D color and surface codes with $d = 5$ under circuit-level depolarizing noise with *sequential* gate execution using a LUT decoder.

VIII. CONCLUSION

In this work, we have introduced automated methods to synthesize (near-)optimal non-deterministic fault-tolerant state preparation circuits for logical computational basis states of any CSS code. We have shown the efficacy of the proposed methods by synthesizing fault-tolerant state preparation circuits for various small CSS codes—relevant for near-term devices—and demonstrated that these circuits have the desired fault-tolerance properties through numerical simulations. Even though we have framed the verification circuit synthesis problem in the context of state preparation of certain logical basis states, our verification circuit synthesis approach is more general. It can be used to verify other circuits as well.

As discussed in Section VI, our methods do not guarantee a globally optimal circuit but rather give locally optimal subcircuits for the state and verification circuit synthesis problems. The natural next step would be to try to unify this into one synthesis problem. Given that

the fault set of the non-fault-tolerant state preparation circuit has a huge impact on the verification circuit, we suspect that there is a large room for improvement, especially when scaling to even higher distances.

In our work, we have assumed all-to-all connectivity between all data and ancilla qubits. Many quantum computing platforms do not provide such lenient locality constraints; however, further steps must be taken to ensure that non-deterministic fault-tolerant state preparation circuits can be embedded into such architectures without sacrificing fault-tolerance.

All in all, this work is an important step towards providing automated design tools for fault-tolerant quantum computing research. The optimized circuits generated by our methods might play a role in further near-term experimental demonstrations of fault-tolerant quantum computing.

IX. USED SOFTWARE

The proposed methods have been implemented using the Python packages Stim [36], NumPy [72], Z3 [57], Qiskit [73], LDPC [74] and Multiprocess [75, 76]. For the simulations we have furthermore used GNU parallel [77]. The plots have been generated with Matplotlib [78].

ACKNOWLEDGMENTS

The authors would like to thank Timo Hillmann for valuable comments on an initial version of the manuscript.

T.P., L.S., L.B., and R.W. acknowledge funding from the European Research Council (ERC) under the European Union’s Horizon 2020 research and innovation program (grant agreement No. 101001318) and Millenion, grant agreement No. 101114305). This work was part of the Munich Quantum Valley, which is supported by

the Bavarian state government with funds from the Hightech Agenda Bayern Plus, and has been supported by the BMWK on the basis of a decision by the German Bundestag through project QuaST, as well as by the BMK, BMDW, and the State of Upper Austria in the frame of the COMET program (managed by the FFG).

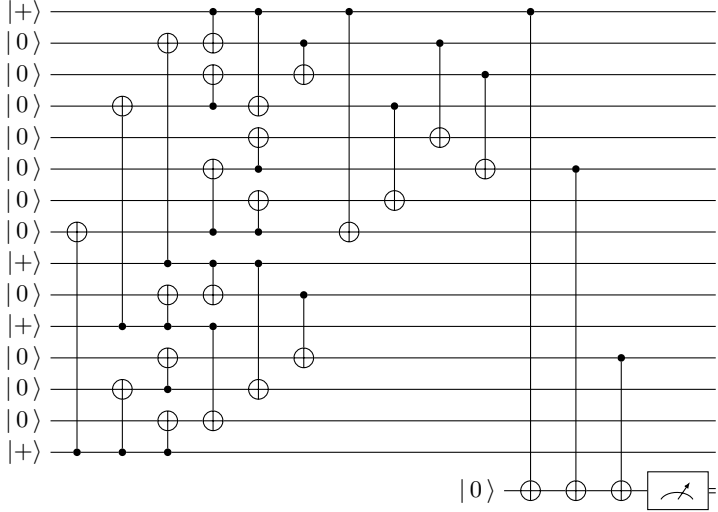
Furthermore, MM gratefully acknowledges support by the European Union’s Horizon Europe research and innovation programme under Grant Agreement No. 101114305 (“MILLENION-SGA1” EU Project) and the ERC Starting Grant QNets through Grant No. 804247. This research is also part of the Munich Quantum Valley (K-8), which is supported by the Bavarian state government with funds from the Hightech Agenda Bayern Plus. He additionally acknowledges support by the BMBF project MUNIQC-ATOMS (Grant No. 13N16070), by the Deutsche Forschungsgemeinschaft (DFG, German Research Foundation) under Germany’s Excellence Strategy “Cluster of Excellence Matter and Light for Quantum Computing (ML4Q) EXC 2004/1” 390534769.

-
- [1] A. R. Calderbank and P. W. Shor, Good quantum error-correcting codes exist, *Phys. Rev. A* **54**, 1098 (1996).
 - [2] A. Steane, Multiple Particle Interference and Quantum Error Correction, *Proc. R. Soc. Lond. A* **452**, 2551 (1996), [arXiv:quant-ph/9601029](#).
 - [3] A. M. Steane, Error Correcting Codes in Quantum Theory, *Phys. Rev. Lett.* **77**, 793 (1996).
 - [4] M. A. Nielsen and I. L. Chuang, *Quantum Computation and Quantum Information* (Cambridge University Press, 2010).
 - [5] N. P. Breuckmann and J. N. Eberhardt, Quantum low-density parity-check codes, *PRX Quantum* **2**, 040101 (2021).
 - [6] H. Bombín, Single-Shot Fault-Tolerant Quantum Error Correction, *Phys. Rev. X* **5**, 031043 (2015).
 - [7] N. Delfosse, B. W. Reichardt, and K. M. Svore, Beyond Single-Shot Fault-Tolerant Quantum Error Correction, *IEEE Trans. Inf. Theory* **68**, 287 (2022).
 - [8] A. O. Quintavalle, M. Vasmer, J. Roffe, and E. T. Campbell, Single-Shot Error Correction of Three-Dimensional Homological Product Codes, *PRX Quantum* **2**, 020340 (2021).
 - [9] O. Fawzi, A. Grospellier, and A. Leverrier, Constant overhead quantum fault tolerance with quantum expander codes, *Commun. ACM* **64**, 106 (2020).
 - [10] H. Goto, Minimizing resource overheads for fault-tolerant preparation of encoded states of the Steane code, *Sci Rep* **6**, 19578 (2016).
 - [11] A. Bermudez, X. Xu, M. Gutiérrez, S. C. Benjamin, and M. Müller, Fault-tolerant protection of near-term trapped-ion topological qubits under realistic noise sources, *Phys. Rev. A* **100**, 062307 (2019).
 - [12] L. Postler, S. Heußen, I. Pogorelov, M. Rispler, T. Feldker, M. Meth, C. D. Marciniak, R. Stricker, M. Ringbauer, R. Blatt, P. Schindler, M. Müller, and T. Monz, Demonstration of fault-tolerant universal quantum gate operations, *Nature* **605**, 675 (2022).
 - [13] C. Chamberland and A. W. Cross, Fault-tolerant magic state preparation with flag qubits, *Quantum* **3**, 143 (2019).
 - [14] F. Butt, S. Heußen, M. Rispler, and M. Müller, Fault-Tolerant Code-Switching Protocols for Near-Term Quantum Processors, *PRX Quantum* **5**, 020345 (2024).
 - [15] S. Heußen, D. F. Locher, and M. Müller, Measurement-Free Fault-Tolerant Quantum Error Correction in Near-Term Devices, *PRX Quantum* **5**, 010333 (2024).
 - [16] C. Ryan-Anderson, J. G. Bohnet, K. Lee, D. Gresh, A. Hankin, J. P. Gaebler, D. Francois, A. Chernoguzov, D. Lucchetti, N. C. Brown, T. M. Gatterman, S. K. Halit, K. Gilmore, J. A. Gerber, B. Neyenhuis, D. Hayes, and R. P. Stutz, Realization of real-time fault-tolerant quantum error correction, *Phys. Rev. X* **11**, 041058 (2021).
 - [17] D. Bluvstein, S. J. Evered, A. A. Geim, S. H. Li, H. Zhou, T. Manovitz, S. Ebadi, M. Cain, M. Kalinowski, D. Hangleiter, J. P. B. Ataiades, N. Maskara, I. Cong, X. Gao, P. S. Rodriguez, T. Karolyshyn, G. Semeghini, M. J. Gullans, M. Greiner, V. Vuletic, and M. D. Lukin, Logical quantum processor based on reconfigurable atom arrays, *Nature* **626**, 58 (2024).
 - [18] M. P. da Silva, C. Ryan-Anderson, J. M. Bello-Rivas, A. Chernoguzov, J. M. Dreiling, C. Foltz, F. Frachon, J. P. Gaebler, T. M. Gatterman, L. Grans-Samuelsson, D. Hayes, N. Hewitt, J. Johansen, D. Lucchetti, M. Mills, S. A. Moses, B. Neyenhuis, A. Paz, J. Pino, P. Siegfried, J. Strabley, A. Sundaram, D. Tom, S. J. Wernli, M. Zaner, R. P. Stutz, and K. M. Svore, **Demonstration of logical qubits and repeated error correction with better-than-physical error rates** (2024), [arXiv:2404.02280](#).
 - [19] I. Pogorelov, F. Butt, L. Postler, C. D. Marciniak, P. Schindler, M. Müller, and T. Monz, **Experimental fault-tolerant code switching** (2024), [arXiv:2403.13732](#).
 - [20] R. Zen, J. Olle, L. Colmenarez, M. Puviani, M. Müller, and F. Marquardt, **Quantum Circuit Discovery for Fault-Tolerant Logical State Preparation with Reinforcement**

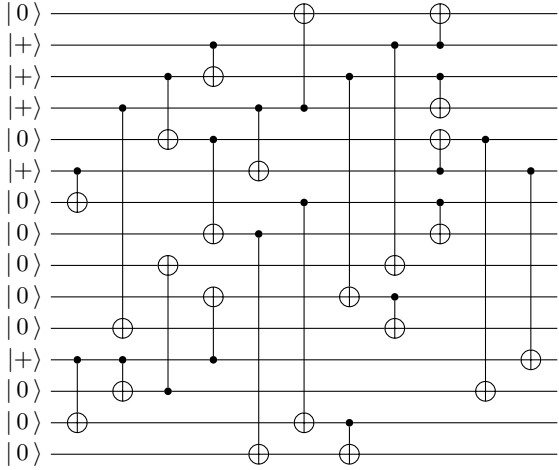
- Learning (2024), [arXiv:2402.17761](https://arxiv.org/abs/2402.17761).
- [21] A. Goswami, M. Mhalla, and V. Savin, Fault-tolerant preparation of quantum polar codes encoding one logical qubit, *Phys. Rev. A* **108**, 042605 (2023).
- [22] A. Goswami, M. Mhalla, and V. Savin, Factory-based fault-tolerant preparation of quantum polar codes encoding one logical qubit, *Phys. Rev. A* **110**, 012438 (2024).
- [23] A. Biere and D. Kröning, SAT-based Model Checking, in *Handbook of Model Checking* (Springer, 2018) pp. 277–303.
- [24] D. Brand, Verification of large synthesized designs, in *Int'l Conf. on CAD* (1993) pp. 534–537.
- [25] S. Eggersglüß, R. Wille, and R. Drechsler, Improved SAT-based ATPG: More constraints, better compaction, in *Int'l Conf. on CAD* (2013).
- [26] A. Gebregiorgis and M. B. Tahoori, Test Pattern Generation for Approximate Circuits Based on Boolean Satisfiability, in *2019 Des. Autom. Test Eur. Conf. Exhib. DATE* (2019) pp. 1028–1033.
- [27] D. Kaufmann, A. Biere, and M. Kauers, Verifying Large Multipliers by Combining SAT and Computer Algebra, in *2019 Form. Methods Comput. Aided Des. FMCAD* (2019) pp. 28–36.
- [28] R. Wille, D. Große, F. Haedicke, and R. Drechsler, SMT-based stimuli generation in the SystemC Verification library, in *Forum on Specification and Design Languages* (2009).
- [29] V. Khomenko, M. Koutny, and A. Yakovlev, Logic synthesis for asynchronous circuits based on Petri net unfoldings and incremental SAT, in *Proc. Fourth Int. Conf. Appl. Concurr. Syst. Des. 2004 ACSD 2004* (2004) pp. 16–25.
- [30] R. Wille, L. Burgholzer, and A. Zulehner, Mapping quantum circuits to IBM QX architectures using the minimal number of SWAP and H operations, in *Design Automation Conf.* (2019).
- [31] B. Tan and J. Cong, Optimal layout synthesis for quantum computing, in *Int'l Conf. on CAD* (2020).
- [32] D. B. Tan, M. Y. Niu, and C. Gidney, A SAT Scalpel for Lattice Surgery: Representation and Synthesis of Subroutines for Surface-Code Fault-Tolerant Quantum Computing (2024), [arXiv:2404.18369](https://arxiv.org/abs/2404.18369) [quant-ph].
- [33] N. Shutty and C. Chamberland, Decoding Merged Color-Surface Codes and Finding Fault-Tolerant Clifford Circuits Using Solvers for Satisfiability Modulo Theories, *Phys. Rev. Applied* **18**, 014072 (2022).
- [34] T. Peham, N. Brandl, R. Kueng, R. Wille, and L. Burgholzer, Depth-Optimal Synthesis of Clifford Circuits with SAT Solvers, in *2023 IEEE Int. Conf. Quantum Comput. Eng. QCE*, Vol. 01 (2023) pp. 802–813.
- [35] S. Schneider, L. Burgholzer, and R. Wille, A SAT encoding for optimal Clifford circuit synthesis, in *Asia and South Pacific Design Automation Conf.* (2023).
- [36] C. Gidney, Stim: a fast stabilizer circuit simulator, *Quantum* **5**, 497 (2021).
- [37] R. Wille, L. Berent, T. Forster, J. Kunasaikaran, K. Mato, T. Peham, N. Quetschlich, D. Rovara, A. Sander, L. Schmid, D. Schönberger, Y. Stade, and L. Burgholzer, The MQT Handbook: A Summary of Design Automation Tools and Software for Quantum Computing (2024), [arXiv:2405.17543](https://arxiv.org/abs/2405.17543).
- [38] D. Gottesman, *Stabilizer codes and quantum error correction.*, Ph.D. thesis, Caltech (1997).
- [39] H. Bombin, *An Introduction to Topological Quantum Codes* (2013), [arXiv:1311.0277](https://arxiv.org/abs/1311.0277).
- [40] P. Aliferis, D. Gottesman, and J. Preskill, Quantum accuracy threshold for concatenated distance-3 codes (2005), [arXiv:quant-ph/0504218](https://arxiv.org/abs/quant-ph/0504218).
- [41] D. Gottesman, *An Introduction to Quantum Error Correction and Fault-Tolerant Quantum Computation* (2009), [arXiv:0904.2557](https://arxiv.org/abs/0904.2557) [quant-ph].
- [42] C. Chamberland and M. E. Beverland, Flag fault-tolerant error correction with arbitrary distance codes, *Quantum* **2**, 53 (2018).
- [43] A. Paetznick and B. W. Reichardt, Fault-tolerant ancilla preparation and noise threshold lower bounds for the 23-qubit Golay code (2013), [arXiv:1106.2190](https://arxiv.org/abs/1106.2190) [quant-ph].
- [44] P.-J. H. S. Derks, A. Townsend-Teague, A. G. Burchards, and J. Eisert, Designing fault-tolerant circuits using detector error models (2024), [arXiv:2407.13826](https://arxiv.org/abs/2407.13826) [quant-ph].
- [45] E. Dennis, A. Kitaev, A. Landahl, and J. Preskill, Topological quantum memory, *Journal of Mathematical Physics* **43**, 4452 (2002).
- [46] A. Kissinger, Phase-free ZX diagrams are CSS codes (..or how to graphically grok the surface code) (2022), [arXiv:2204.14038](https://arxiv.org/abs/2204.14038) [quant-ph].
- [47] J. Jiang, X. Sun, S.-H. Teng, B. Wu, K. Wu, and J. Zhang, Optimal Space-Depth Trade-Off of CNOT Circuits in Quantum Logic Synthesis (2022), [arXiv:1907.05087](https://arxiv.org/abs/1907.05087) [quant-ph].
- [48] K. N. Patel, I. L. Markov, and J. P. Hayes, Optimal synthesis of linear reversible circuits, *Quantum Info. Comput.* **8**, 282 (2008).
- [49] D. Maslov and B. Zindorf, Depth Optimization of CZ, CNOT, and Clifford Circuits, *IEEE Trans. Quantum Eng.* **3**, 1 (2022).
- [50] Timothée Goubault de Brugière, M. Baboulin, B. Valiron, S. Martiel, and C. Allouche, Gaussian Elimination versus Greedy Methods for the Synthesis of Linear Reversible Circuits, *ACM Transactions on Quantum Computing* **2**, 1 (2021).
- [51] S. Bravyi, J. A. Latone, and D. Maslov, 6-qubit optimal Clifford circuits, *npj Quantum Inf* **8**, 1 (2022).
- [52] S. Aaronson and D. Gottesman, Improved simulation of stabilizer circuits, *Phys. Rev. A* **70**, 052328 (2004).
- [53] S. Bravyi, R. Shaydulin, S. Hu, and D. Maslov, Clifford circuit optimization with templates and symbolic Pauli gates, *Quantum* **5**, 580 (2021), [arXiv:2105.02291](https://arxiv.org/abs/2105.02291).
- [54] D. Maslov, Linear Depth Stabilizer and Quantum Fourier Transformation Circuits with no Auxiliary Qubits in Finite Neighbor Quantum Architectures, *Phys. Rev. A* **76**, 052310 (2007).
- [55] V. Kabanets and J.-Y. Cai, Circuit minimization problem, in *Proc. Thirty-Second Annu. ACM Symp. Theory Comput.* (ACM, 2000) pp. 73–79.
- [56] A. Biere, M. Heule, Hans van Maaren, and T. Walsh, *Handbook of Satisfiability* (IOS Press, 2009).
- [57] Leonardo de Moura and N. Björner, Z3: An efficient SMT solver, in *Tools Algorithms Constr. Anal. Syst.* (Springer, 2008) pp. 337–340.
- [58] B. Schaeffer and M. Perkowski, A Cost Minimization Approach to Synthesis of Linear Reversible Circuits (2014), [arXiv:1407.0070](https://arxiv.org/abs/1407.0070).
- [59] E. Berlekamp, R. McEliece, and H. van Tilborg, On the Inherent Intractability of Certain Coding Problems, *IEEE Trans. Inf. Theory* **24**, 384 (1978).
- [60] R. M. Karp, Reducibility among Combinatorial Problems, in *Complexity of Computer Computations: Pro-*

- ceedings of a symposium on the Complexity of Computer Computations, held March 20–22, 1972, at the IBM Thomas J. Watson Research Center, Yorktown Heights, New York, and sponsored by the Office of Naval Research, Mathematics Program, IBM World Trade Corporation, and the IBM Research Mathematical Sciences Department*, edited by R. E. Miller, J. W. Thatcher, and J. D. Bohlinger (Springer US, Boston, MA, 1972) pp. 85–103.
- [61] V. Chvatal, A Greedy Heuristic for the Set-Covering Problem, *Math. Oper. Res.* **4**, 233 (1979).
- [62] M. Borges-Quintana, M. A. Borges-Trenard, and E. Martínez-Moro, [Computing coset leaders of binary codes](#) (2010), [arXiv:1001.5074](#).
- [63] M. Borges-Quintana, M. A. Borges-Trenard, I. Márquez-Corbella, and E. Martínez-Moro, [Computing coset leaders and leader codewords of binary codes](#) (2014), [arXiv:1211.5568](#).
- [64] E. W. Mayr, Some Complexity Results for Polynomial Ideals, *Journal of Complexity* **13**, 303 (1997).
- [65] R. Chao and B. W. Reichardt, Flag Fault-Tolerant Error Correction for any Stabilizer Code, *PRX Quantum* **1**, 010302 (2020).
- [66] A. Steane, Quantum Reed-Muller codes, *IEEE Trans. Inf. Theory* **45**, 1701 (1999).
- [67] P. W. Shor, Scheme for reducing decoherence in quantum computer memory, *Phys. Rev. A* **52**, R2493 (1995).
- [68] H. Bombin and M. A. Martin-Delgado, Optimal resources for topological two-dimensional stabilizer codes: Comparative study, *Phys. Rev. A* **76**, 012305 (2007).
- [69] A. M. Steane, Simple quantum error-correcting codes, *Phys. Rev. A* **54**, 4741 (1996).
- [70] H. Bombin and M. A. Martin-Delgado, Topological Quantum Distillation, *Phys. Rev. Lett.* **97**, 180501 (2006).
- [71] S. J. Evered, D. Bluvstein, M. Kalinowski, S. Ebadi, T. Manovitz, H. Zhou, S. H. Li, A. A. Geim, T. T. Wang, N. Maskara, H. Levine, G. Semeghini, M. Greiner, V. Vuletić, and M. D. Lukin, High-fidelity parallel entangling gates on a neutral-atom quantum computer, *Nature* **622**, 268 (2023).
- [72] C. R. Harris, K. J. Millman, S. J. van der Walt, R. Gommers, P. Virtanen, D. Cournapeau, E. Wieser, J. Taylor, S. Berg, N. J. Smith, R. Kern, M. Picus, S. Hoyer, M. H. van Kerkwijk, M. Brett, A. Haldane, J. F. del Río, M. Wiebe, P. Peterson, P. Gérard-Marchant, K. Sheppard, T. Reddy, W. Weckesser, H. Abbasi, C. Gohlke, and T. E. Oliphant, Array programming with NumPy, *Nature* **585**, 357 (2020).
- [73] Qiskit contributors, [Qiskit: An Open-source Framework for Quantum Computing](#), Zenodo (2023).
- [74] J. Roffe, [LDPC: Python tools for low density parity check codes](#) (2022).
- [75] M. M. McKerns, L. Strand, T. Sullivan, A. Fang, and M. A. G. Aivazis, [Building a Framework for Predictive Science](#) (2012), [arXiv:1202.1056](#).
- [76] Michael McKerns and Michael Aivazis, [pathos: a framework for heterogeneous computing](#) (2010).
- [77] O. Tange, *GNU Parallel 2018* (Ole Tange, 2018).
- [78] J. D. Hunter, Matplotlib: A 2D graphics environment, *Comput. Sci. Eng.* **9**, 90 (2007).

Appendix A: Circuits



(a) Non-deterministic fault-tolerant $|0\rangle_L$ of the $[[15, 1, 3]]$ code



(b) fault-tolerant $|+\rangle_L$ of the $[[15, 1, 3]]$ code. No verification circuit is required.

FIG. 12: fault-tolerant state preparation circuits for the $[[15, 1, 3]]$ “tetrahedral” code.

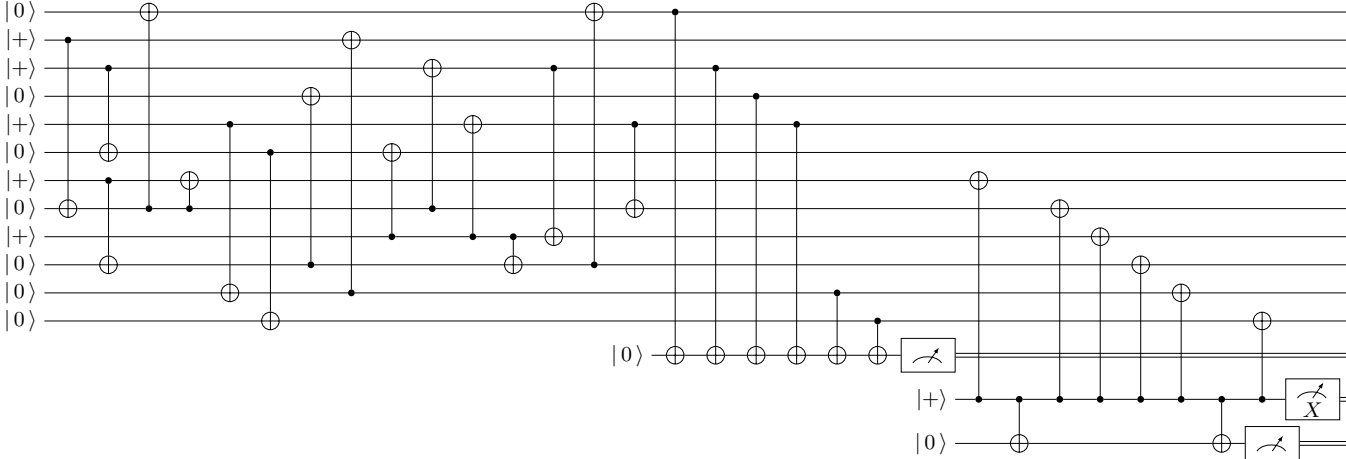


FIG. 13: Non-deterministic fault-tolerant $|0\rangle_L^2$ of the $[[12, 2, 4]]$ “Carbon” code.

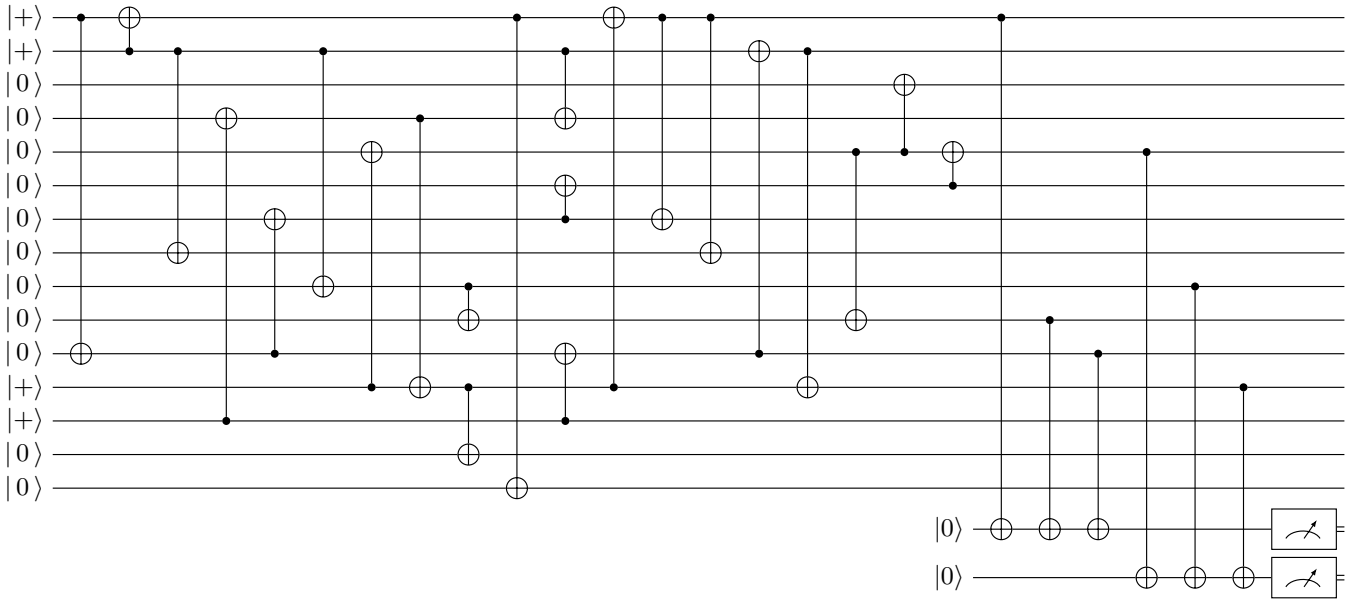


FIG. 14: Non-deterministic fault-tolerant $|0\rangle_L^7$ of the $[[15, 7, 3]]$ Hamming code.

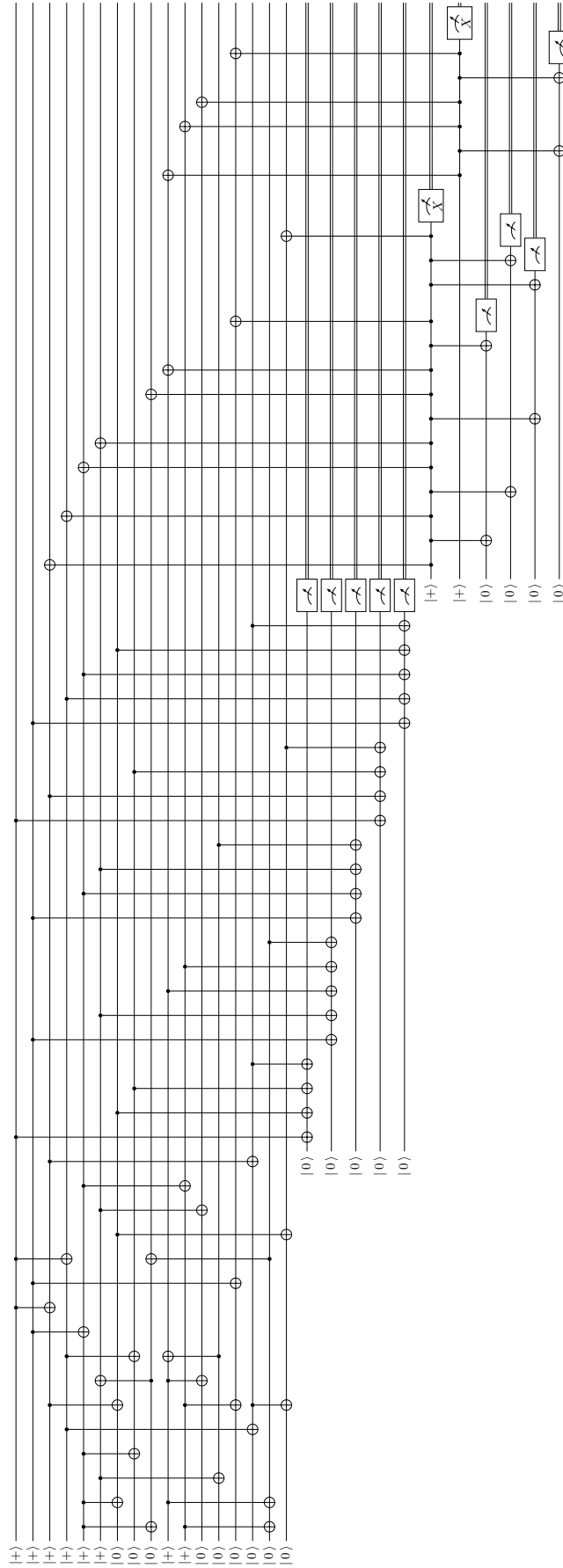


FIG. 15: Non-deterministic fault-tolerant $|0\rangle_L$ of the $[[17, 1, 5]]$ code.

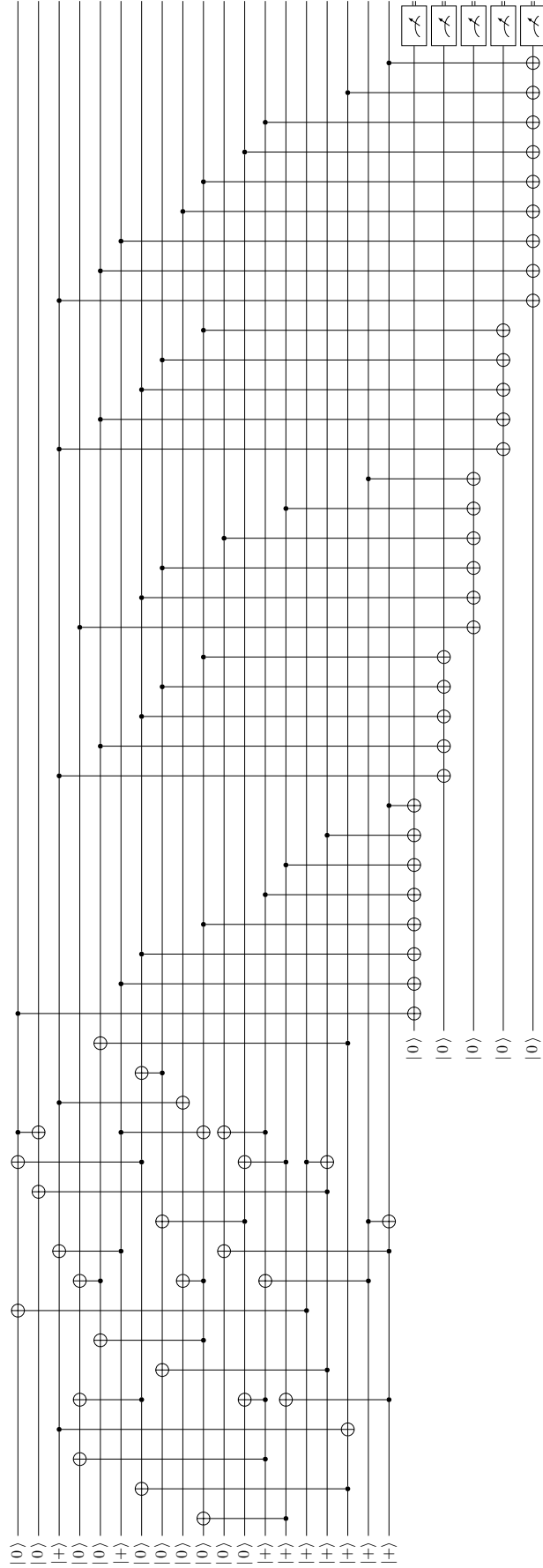


FIG. 16: Non-deterministic fault-tolerant $|0\rangle_L$ of the $[[19, 1, 5]]$ color code. Here only verification for X errors is shown.